

**PROPOSAL OF A NOVEL METHOD FOR OSCILLATING IPMCS WITH  
DC INPUT**

Louise Penna Poubel

Chiba University  
Chiba, Japan  
February 2011

## ABSTRACT

Ionic polymer-metal composites (IPMCs) are materials with inherent actuation and sensing functions which have great potential to be used in active materials systems. IPMCs are electro-active polymers, undergoing bending deformation under electrical inputs of a few volts (1V to 4V) due to the electro-osmosis of freely moving ions in the polymer membrane.

Applications proposed for IPMCs in the literature have in common that the driving circuitry is fixed against the actuator throughout the whole usage and requires an AC input to generate oscillation. In this research, a novel approach is attempted which uses the actuator's own movement to switch the voltage being applied across it.

A cantilever configuration is studied in which the actuator is fixed to the anode and only touching the cathode. Under a step input the actuator bends towards the anode and loses connection with the cathode turning off the input across itself. The actuator then returns elastically to the cathode starting another cycle. This configuration performs oscillation under a 3V step input in air. Two different materials are tested as the cathode, aluminum and copper. The former presents less oscillation stability than the latter.

The copper cathode is pressed against the actuator at different positions along the axis orthogonal to the actuator. More pressed positions present longer first impulses and higher origin shifts. Two types of oscillation are observed, cyclic and continuous. Less pressed cathode positions present cyclic oscillation, intermediary positions transition from cyclic to continuous oscillations and for more pressed positions the actuator performs continuous oscillations from the start.

Cyclic oscillation frequency increases with time for all cathode positions. For positions which didn't transition, the frequency stays below 2 Hz during the observed time. Positions which transition have cyclic frequencies quickly rising from around 1.5 Hz to almost 5 Hz. The frequency of unforced oscillations in each cycle also increases with time and is around 30 Hz for all positions. The first amplitude in a cycle increases with the effective voltage applied on the actuator. The lower the first amplitude is the more impulses are received until a cycle ends. Impulses following the first one increase the amplitude and consecutive

impulses tend to counter damping and maintain the previous amplitude.

The frequency of continuous oscillations increases with time as well, ranging from 31 Hz to 66 Hz with dehydration. The continuous amplitude decreases as the frequency increases and it decays with time. The amplitudes obtained with the newly presented DC input approach present amplitudes comparable to those of AC-driven systems for the same frequency range.

## Outline

This paper will describe a novel concept in actuating recently developed materials called ionic polymer-metal composites (IPMCs). A specific configuration which has the potential of performing oscillation making use of a DC input using the new concept will be experimentally tested and the obtained results discussed upon.

In Chapter 1 there will be an introduction to the growing field of smart materials and active materials systems. Section 1.1 will introduce the smart material used in this research; Section 1.2 will discuss the current applications for this material; Section 1.3 will introduce the novel approach and Section 1.4 will present the specific case which will be analyzed in this paper.

Chapter 2 will present preliminary experiments performed as a foundation for the main experiments which will be described in Chapter 3. Section 2.1 will describe the specimen used and the experimental conditions which were tested in the attempt of obtaining oscillation; Section 2.2 will discuss the effects of two different electrode materials on oscillation as well as some characteristics of the oscillation.

Chapter 3 will explain the main experiments performed to compare the influence of cathode position in oscillation. Section 3.1 will describe the improvements in relation to previous experiments in the experimental setup. In Section 3.2 the obtained results will be discussed in the following order: Section 3.2.1 will discuss the first few seconds of oscillation; Section 3.2.2 will discuss the characteristics of the two main types of oscillation; Section 3.2.3 will compare the oscillations obtained with the new approach to oscillations obtained in the traditional method in the same frequency range.

In Chapter 4, alternative configurations using the novel approach will be introduced. And Chapter 5 will conclude the research and talk about future research.

## Table of Contents

### Chapter 1 Introduction

- 1.1 Active Materials Systems
- 1.2 Introduction to Ionic Polymer-Metal Composites (IPMCs)
- 1.3 Current usage of IPMCs
- 1.4 Novel approach to the actuation of IPMCs
- 1.5 Specific configuration to be analyzed

### Chapter 2 Effects of cathode material on oscillation

- 2.1 Introduction
- 2.2 Experimental setup
- 2.3 Results and discussion
- 2.4 Conclusion

### Chapter 3 Effects of cathode position on oscillation

- 3.1 Introduction
- 3.2 Experimental setup
- 3.3 Results and discussion
  - 3.3.1 Initial response analysis
  - 3.3.2 Oscillation analysis
    - 3.3.2.1 Cyclic oscillation
    - 3.3.2.2 Continuous oscillation
  - 3.3.3 Comparison with a traditional sine input

### Chapter 4. Other configurations using the novel approach

- 4.1 Introduction
- 4.2 Non-fixed pumping
- 4.3 Actuator between walls with a potential across them
- 4.4 Triple-snap
- 4.5 Free bender
- 4.6 Bias structure

Chapter 5. Conclusions

References

Acknowledgements

## Chapter 1 Introduction

### 1.1 Active Materials Systems

Traditional mechanisms are composed of various elements which work together to perform specific functions. Some elements are structural, others perform actuation, sensing, etc. These systems are limited in their applications, for each new element inserted to perform one single function brings inconveniences such as extra need for space and power, generation of noise, electromagnetic fields and others. Recently the field of smart materials has been receiving increased attention for promising alternatives to overcome some of the limitations of traditional systems.

Smart materials are those which respond directly to changes in their surroundings with some form of useful response. For example, electro-active polymers (EAPs) are materials which respond to electric inputs with mechanical deformation <sup>1)</sup>. Other kinds of smart materials include piezoelectric materials, shape memory alloys, active laminates, etc <sup>1-2)</sup>. Much effort is being put into combining smart materials to form active materials systems which perform multiple functions as illustrated in Fig. 1.1 to optimize mechanical systems.

### 1.2 Introduction to Ionic Polymer-Metal Composites (IPMCs)

IPMCs consist of an ionic polymer membrane (also known as ion-exchange membrane, IEM) plated with noble metal on both surfaces. The porous membrane is ionized with anions covalently fixed to the backbone and filled with freely moving cations (or cationic groups) to balance the charge together with a polar solvent (usually water). The metal layers work as electrodes, so when there's a voltage gradient across them, the cations get pulled towards the cathode dragging water molecules along with them (pumping effect). This electro-kinetic phenomenon called electro-osmosis results in pressure gradients across the membrane which force the actuator to bend towards the anode, as illustrated in

Fig. 1.2 <sup>3-5)</sup>.

Its direction and amplitude of response are proportional to the input voltage, so applying an alternating voltage results in oscillatory bending <sup>4)</sup>. IPMCs respond to low voltages (1V to 4V), but voltages higher than 1.5V give rise to water electrolysis, generating bubbles <sup>6)</sup>.

The ionic polymer membrane used in these actuators is usually Nafion or Flemion. The noble metal used on the electrode layers is typically gold or platinum, the earlier being less rigid and more conductive than the latter <sup>7)</sup>. IPMCs are isotropic, bending equally on all directions; by choosing a large aspect ratio, the bending of most directions can be neglected in relation to the longer one.

Water molecules carried along the cations consist of the main mechanism of actuation, especially in the case of small ions. Under step inputs, although ions remain within the boundary layer, water molecules which were initially dislocated slowly return giving rise to a phenomenon known as back-relaxation <sup>5)</sup>. When these composites are used in air, water evaporation decreases performance with time <sup>4)</sup>. Various ways of overcoming this problem have been proposed in the literature, such as the use of ionic liquids as the solvent or encapsulation processes to keep water from evaporating. Both of these approaches have been shown to slow down the response of the actuator however <sup>4,23)</sup>.

It is known that the positive counter-ion used to dope the membrane affects the displacement response of the actuator as what's called the doping effect. Smaller ions such as alkali metals offer little resistance while moving through the porous backbone and therefore current runs instantly and response is faster than for bigger ions. Also, for small ions, higher back relaxation is observed, because the water molecules which had been carried along can return easily <sup>5,7-8)</sup>.

A secondary actuation mechanism is due to the coulombian interactions between the negative backbone and the charges on the dendritic electrode layers <sup>5)</sup>. There are various phenomena overlapped in the actuation of IPMCs, and their movement is nonlinear, especially at lower frequencies. There's no widely accepted model to their actuation yet; it is widely accepted however that their response is capacitive, with lower currents at lower frequencies and presenting hysteresis <sup>9)</sup>.

Indeed, there are researchers focusing on increasing the capacitive properties of IPMCs to use them as soft capacitors which come in various sizes<sup>10)</sup>.

Compared to traditional mechanisms and other smart materials, IPMCs perform large motion, are lightweight, can be easily miniaturized, and have a high force output to weight ratio, being able to support over 40 times their own weight<sup>4)</sup>. Moreover, they are soft materials which perform biomimetic actuation. However, several problems have to be solved before they can be used in real applications, including their low repeatability, lack of long-term stability and inherent imperfections due to the current state of the manufacturing processes<sup>9,11-12)</sup>.

A lot of progress has been achieved since IPMCs were first developed in 1992 by Oguro et al.<sup>13)</sup>, such as the development of novel polymers and dopants, increase of durability, electrode patterning and shape molding<sup>14-16)</sup>. It's also worth mentioning that IPMCs possess inherent sensing functions, providing an electric output in the order of microvolt's proportional to the direction and amplitude of suffered mechanical deformations<sup>17)</sup>. Some researchers are also investigating ways to use the change in resistance on the surface electrodes to sense the actuator's movement<sup>18)</sup>. All these characteristics make of IPMCs great candidates for becoming multi-functional materials in several applications.

### 1.3 Current usage of IPMCs

Some applications developed for IPMCs are shown in Fig. 1.3. Applications under development include biomimetic robots<sup>4,6,12,15,16,19-21)</sup>, manipulators<sup>4)</sup>, micro-pumps<sup>22)</sup>, active catheters<sup>23)</sup> and vibration damping<sup>17)</sup>. While most researchers have focused on controlling IPMCs by changing the input voltage, some have made use of a lack of electrochemical equilibrium to obtain oscillations<sup>24-25)</sup>. Whether driven by AC inputs or chemical oscillations, in all the applications found in the literature, the actuators were fixed against the conditioning circuitry during the whole usage.

Researchers have pointed out that in several cases, bulky electronics take

away many of the advantages of IPMCs, such as lightweight and compactness, holding up the development of autonomous devices<sup>19)</sup>. Especially in the case of self-actuated structures, where IPMCs are expected to act as structural and actuation elements at once (because they can easily carry their own weight), the need for wires connecting to external circuitry greatly limits the movement of such structures<sup>12)</sup>.

#### 1.4 Novel approach to the actuation of IPMCs

A novel approach to the actuation of IPMCs will be focused on in the present research. The IPMC's need for energy to maintain a constant position has been repeatedly described in the literature as a drawback to the use of these materials compared to other smart materials<sup>11)</sup>. Looking from another angle however, the IPMC's tendency to return to an equilibrium position could be useful in the creation of new mechanisms which use energy more efficiently and require simpler circuitry.

The general concept to be investigated here is to use the IPMC's own movement to switch the voltage applied across it, alternating electrical and mechanical forces to generate oscillation. A step input bends the actuator until it loses contact with the electrode which powered it. From the moment contact is lost the IPMC elastically returns to equilibrium starting a new cycle. To the best of our knowledge, no researchers have tackled this approach yet.

For being soft materials, much has been said about their advantages in interacting with environmental dynamics and using their elasticity, flexibility and back-drivability in increasing efficiency<sup>4,20,21,26)</sup>. The novel approach presented here has a great potential of taking advantage of these characteristics. Additionally, since this angle has never been tried before, this approach might contribute to new understandings of these actuators.

The long term objectives of this research are to eliminate the need for complex electronics when performing oscillation, to eliminate the need for restraining connections, to embed these actuators into structures which have constant

potentials across them, to obtain actuation from direct interaction with mechanical systems and to combine these actuators with thin film batteries to make unrestrained lightweight moving devices.

In the present preliminary study, the feasibility of such mechanisms is examined. It is checked whether the IPMC can separate from the electrode where it got power from. When that's possible, it is checked if oscillation is possible.

## 1.5 Specific configuration to be analyzed

A configuration is investigated where the actuator strip is placed as a cantilever fixed to the anode on one side and touching the cathode on the other as shown in Fig. 1.4. When receiving an electrical input, the actuator bends towards the anode and "jumps" away from the cathode. As contact with the cathode is lost, no voltage is applied to the actuator anymore, so it returns to the cathode starting another cycle.

In this configuration, the anode is fixed to the IPMC throughout the whole actuation as in traditional systems. Contact with the cathode however is lost when the actuator bends away, so the actuator's own movement switches off the voltage across it. Here, the cathode acts as a mechanical constraint as well, allowing the beam to move freely only to one of its sides.

This configuration offers the possibility of separation between the actuator and one of its powering electrodes, as well as the possibility of obtaining oscillation from a DC input, considerably simplifying circuitry in relation to traditional systems. Different from alternating input-controlled configurations however, this system does not offer electrical controllability during the application, as most of the parameters defining the movement's characteristics are related to the mechanical configuration.

After testing various conditions in order to obtain oscillation, such as the environment of the experiment, the material of the electrodes and the size of the actuator, this research is focused on characterizing the resulting oscillation for different cathode positions.

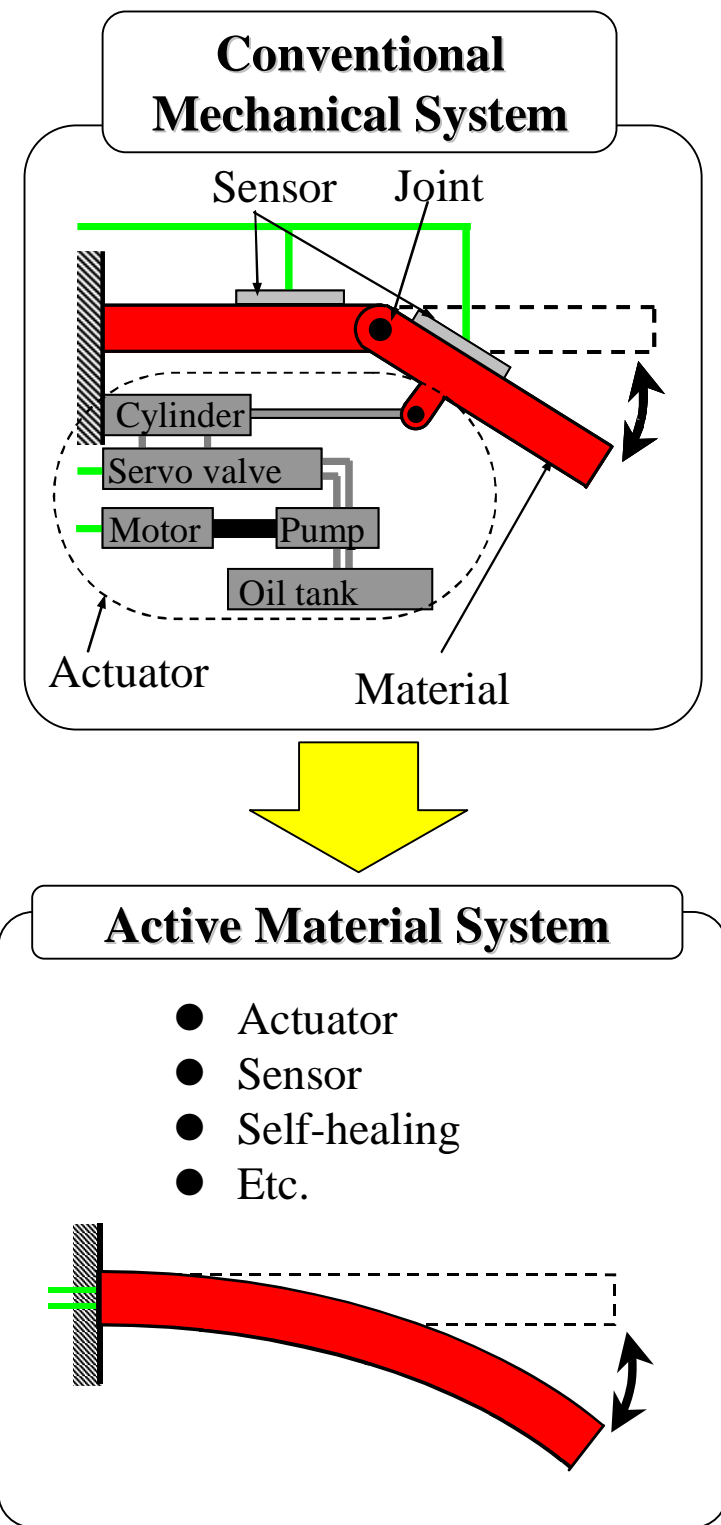


Fig. 1.1 Comparison between a conventional mechanical system and an active material system

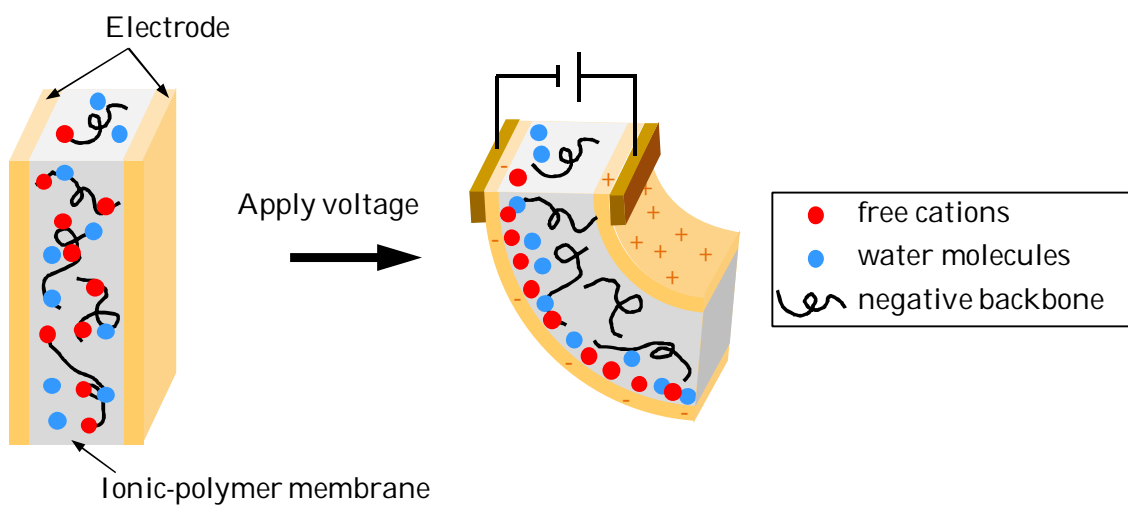


Fig. 1.2 IPMC's actuation principle

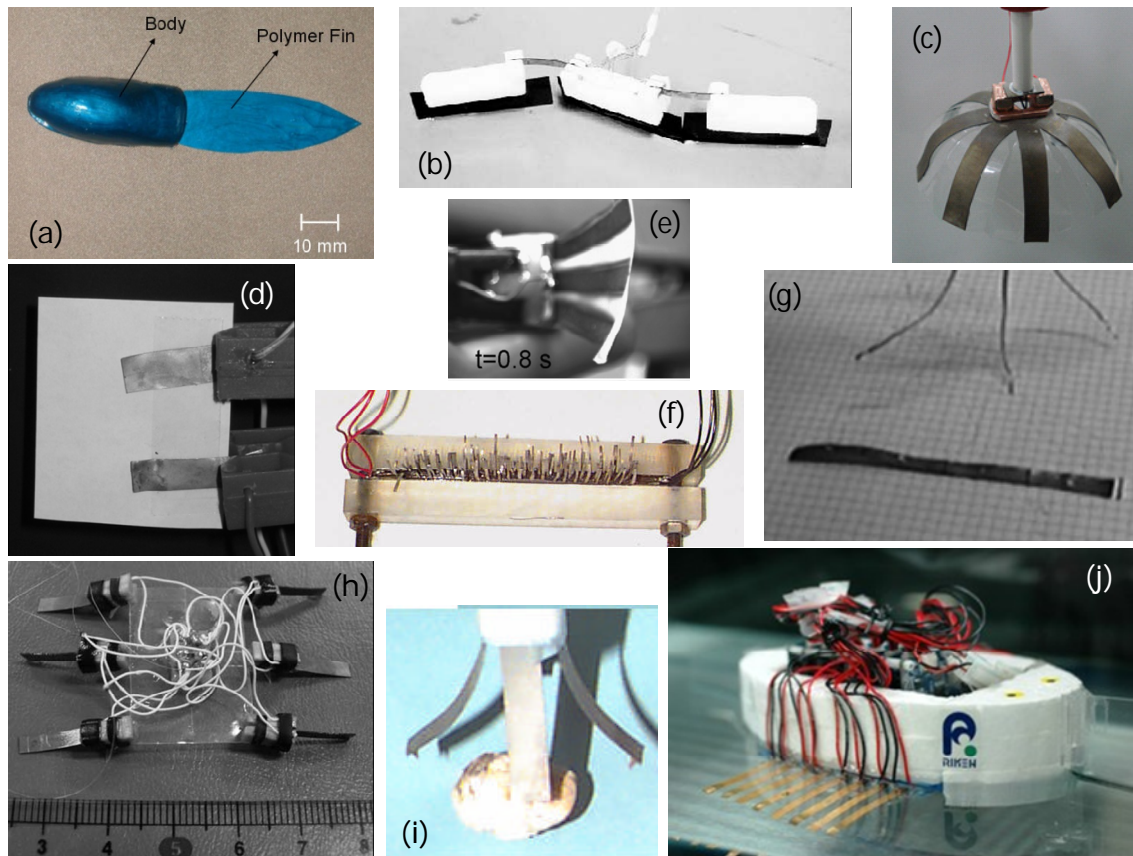


Fig. 1.3 Examples of the current usage of IPMCs: (a) tadpole <sup>19)</sup>, (b) snake-like robot <sup>21)</sup>, (c) jellyfish <sup>16)</sup>, (d) sensor-actuator vibration control <sup>17)</sup>, (e) fish fin <sup>14)</sup>, (f) cilia <sup>4)</sup>, (g) wormlike robot <sup>12)</sup>, (h) hybrid fish-like robot <sup>6)</sup>, (i) gripper <sup>4)</sup>, (j) autonomous rajiform robot <sup>20)</sup>

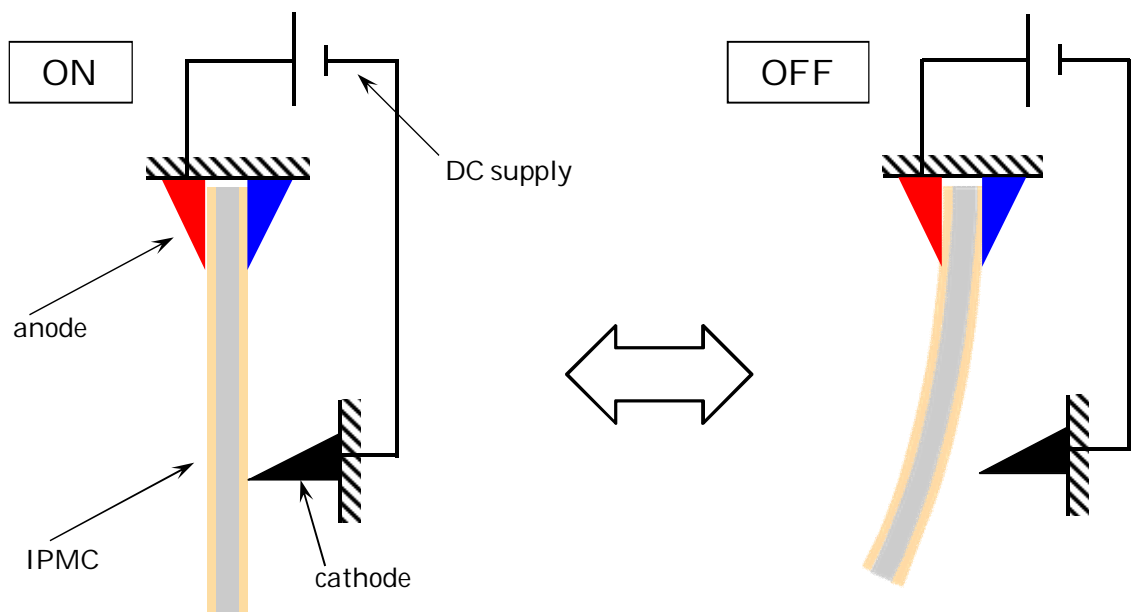


Fig. 1.4 Novel configuration's actuation principle

## Chapter 2 Effects of cathode material on oscillation

### 2.1 Introduction

This chapter will explain the progress of the preliminary attempts to obtain oscillation using the novel configuration previously described. The experimental conditions attempted will be described and the results for two different cathode materials discussed.

### 2.2 Experimental setup

The IPMC specimen used in this experiment was prepared at the National Institute of Advanced Industrial Science and Technology by the chemical plating method described in <sup>3)</sup>. The ionic polymer membrane is a Nafion 117 film, the electrode layers are made of gold and the counter-ion used is Na<sup>+</sup>. For this experiment, the long strip measuring 5 × 27 mm shown in Fig. 2.1 was cut from the prepared sample and has an average thickness of 0.2 mm.

Experiments were attempted in water but no oscillation could be observed. Moreover, for higher voltages, water electrolysis gave rise to bubbles which accumulated under the actuator and the cathode disturbing movement. Thus it was decided to conduct further experiments in air as commonly found in the literature <sup>4,9)</sup>.

The current state-of-the-art IPMCs still present low repeatability and low long-term stability. One widely used method of neutralizing the membrane to recreate similar conditions between experiments performed in air is to insert the specimen in water for at least 30 minutes between experiments, so this approach was performed here as well <sup>4,9)</sup>.

The experimental setup is shown in Fig. 2.2 and a scheme of it in Fig. 2.3. The specimen was supported vertically by a clamp covered with copper films on both sides which provide individual electrical connection to each of the actuator's surfaces. A 3mm length was fixed in the clamp leaving 24mm of free beam.

While the electrode in the clamped end was made of copper, two different materials were experimented for the non-fixed electrode. The bars of aluminum and copper used as cathodes are seen in Fig. 2.4. Wires were soldered on the copper cathode for connection and glued with silver paste and epoxy on the aluminum one. The bars have cross sections measuring  $1 \times 2$  mm. Different shapes of cathodes were considered; this one was chosen for being shorter than the width of the IPMC and not too small, having a sharp edge, providing good contact and assurance of where contact is happening.

The cathode is placed with its largest surface facing the top of an x-y-z stage, touching the IPMC at a distance of 12 mm from the actuator's tip, which is the center of the free beam, at the center of the actuator's width.

Before applying the input voltage, the cathode is pressed against the actuator to assure there's contact between them. The input of 3 V is applied through the anode fixed in the clamp and the non-fixed cathode. A multifunction generator WF1974 connected to a HSA4051 high speed bipolar amplifier was used to apply the input. The displacement was measured at 4mm above the actuator's tip by a KEYENCE LB-1100/080 laser displacement sensor and recorded by a YOKOGAWA DL1640 digital oscilloscope. Simultaneously, the input voltage and the voltage across the membrane were recorded by the oscilloscope.



Fig. 2.1 Specimen's appearance

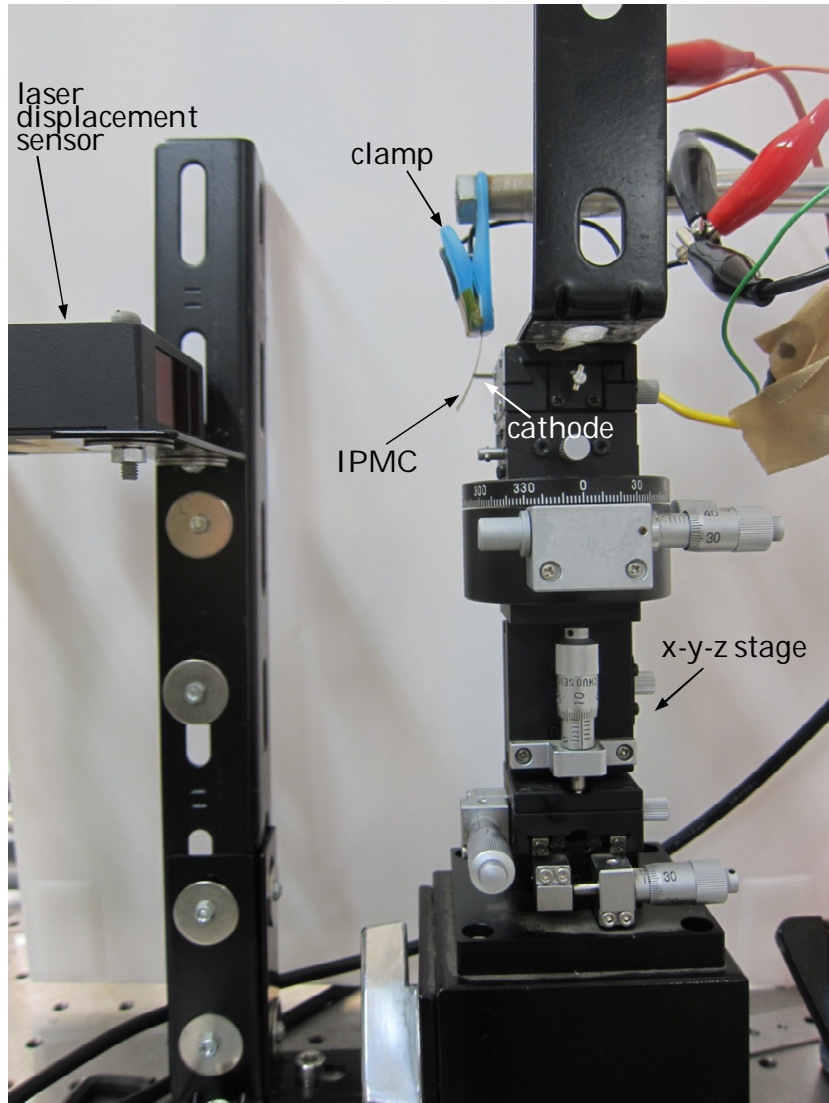
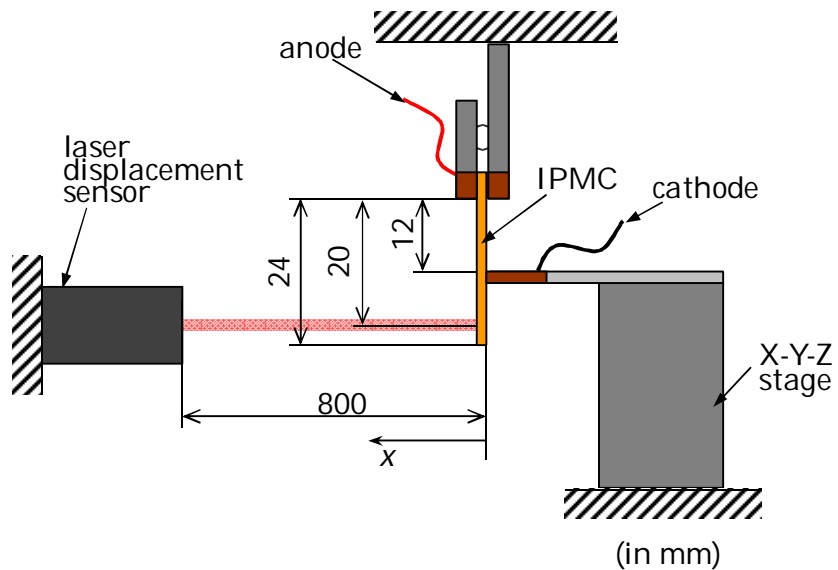
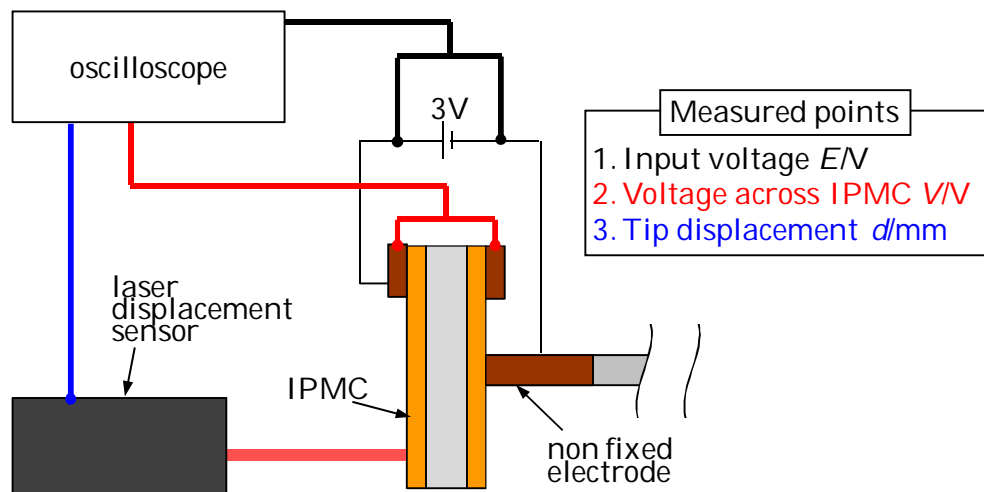


Fig. 2.2 Oscillation measurement system.



(a) Conditions



(b) Measurement points

Fig. 2.3 Schematic diagram of the oscillation measurement system.



(a) copper



(b) aluminum

Fig. 2.4 Metal bars used as cathodes

## 2.3 Results and discussion

The voltage across the IPMC and tip displacement observed for the copper cathode and the aluminum cathode are shown in Fig. 2.5 and Fig. 2.6 respectively.

When the IPMC is touching the cathode the circuit is closed, so the voltage across the actuator gets close to the 3 V input, and when separation happens and the circuit opens, the voltage read across the actuator is that which was charged between its electrode layers. This confirms that separation occurred. The time of contact is quicker than the time separated in both cases.

Furthermore, as we can see by the repetitive tip displacements, it was confirmed that oscillation is achieved for both cathodes. It is also worth noticing that the IPMC was moving erratically before input was applied. Moreover, it is visible that the amplitude of oscillation varies throughout time, as well as the position of the origin of oscillation.

At times the voltage across the actuator appears to increase suddenly without having touched the cathode, this is because the oscilloscope's sampling rate of 50 ms wasn't fast enough to register the quick time of contact (this problem was solved in the subsequent experiments).

The voltage across the actuator increases with time and eventually reaches the input value for the copper cathode, what will be referred to as *voltage saturation* and poses a challenge to long-term stability of this configuration. Voltage increase is balanced by voltage leakage to a certain extent, this will be discussed in the following chapter.

The voltage for the aluminum cathode rises more slowly and gets erratic towards the end. However, even though voltage shows that the actuator is separating from the electrode, the amplitude of oscillation is negligible for most of the experiment. On the other hand, the tip displacement for the copper cathode is more consistent throughout the experiment.

A possible reason for the bad performance of the aluminum cathode could be corrosion on the aluminum cathode's surface due to the water in the IPMC disrupting connection.

## 2.4 Conclusion

When aluminum was used in the cathode, the electrical contact surface became less conductive with time and unsettled oscillations. These results show that copper is a more suitable material for the non-fixed electrode than aluminum.

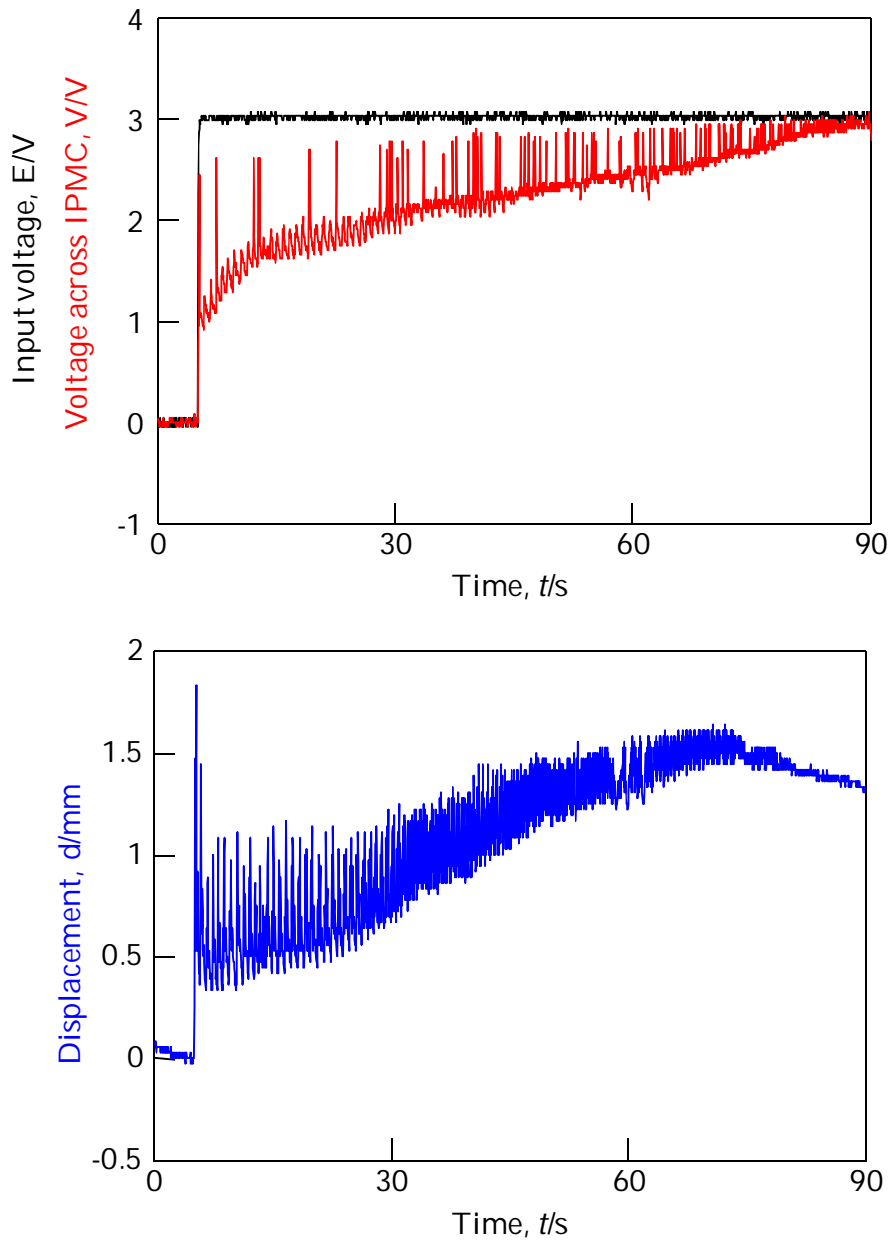


Fig. 2.5 Voltage across the actuator and tip displacement for copper electrode

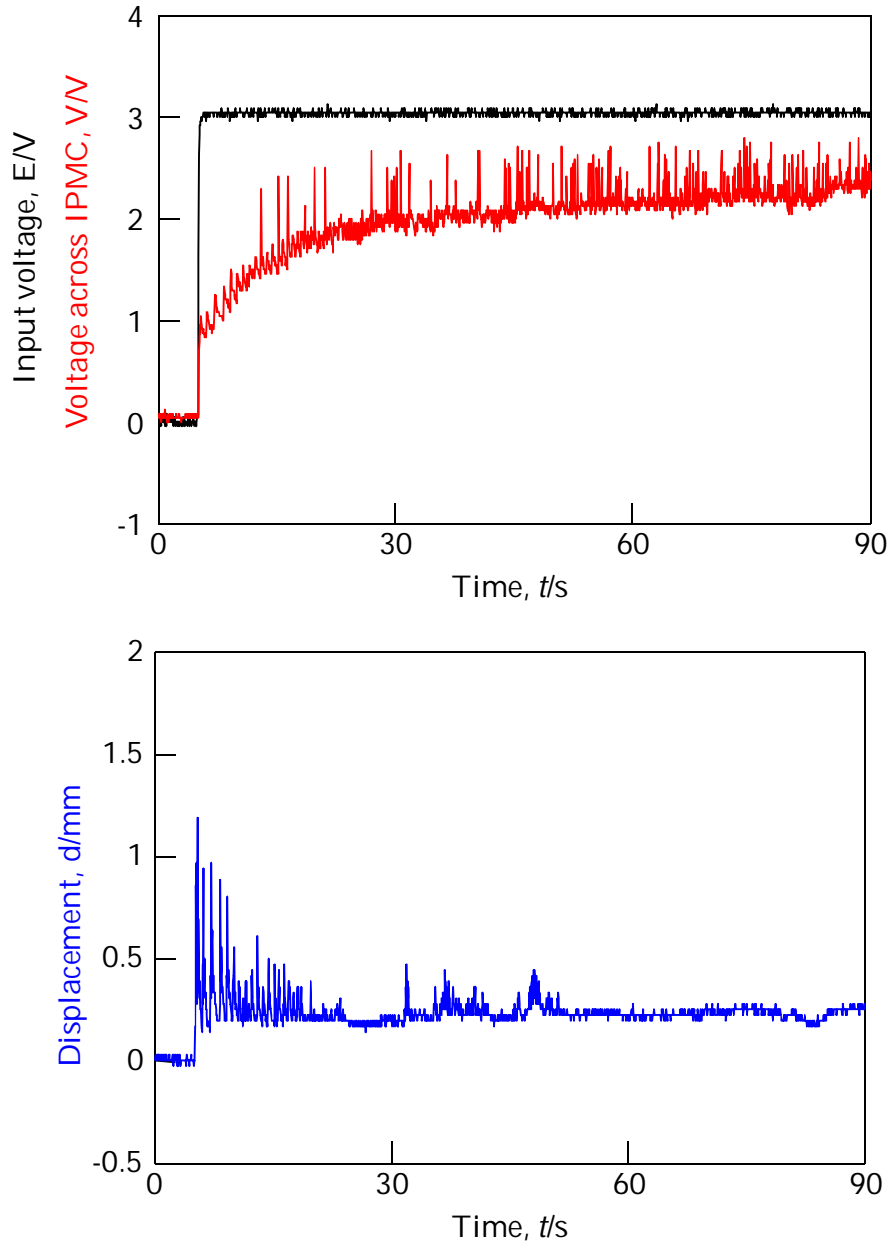


Fig. 2.6 Voltage across the actuator and tip displacement for aluminum electrode

## Chapter 3 Effects of cathode position on oscillation

### 3.1 Introduction

In this chapter, experiments are performed with the copper electrode in a fixed vertical position and in different positions along the x axis. The main characteristics of the resulting oscillations and the effects of the cathode position on them will be discussed.

### 3.2 Experimental setup

The specimen used in this experiment is cut in the same size (27 mm × 5mm × 0.2 mm) from the same original sheet as the specimen in the previous experiment as recommended in the literature <sup>23)</sup>. As said earlier, due to imperfections during the manufacturing process, actuators with similar measures can have considerably different responses even if they come from the same sheet. To increase repeatability and allow comparison, all experiments in this chapter are performed with the same specimen.

The IPMC was fixed the same way as before, but this time, the actuator was inserted into water in between experiments without being removed from the setup. Before and after each experiment a sine wave of ±3 V in 0.5 Hz is applied to the specimen in order to induce even stresses and redistribute the molecules inside the membrane. Each experiment was performed according to the timing in Fig. 3.1 in air, at a room temperature of around 18 °C and humidity of around 28 %.

A total of 13 different positions along the x axis are investigated, every 0.2 mm from 0.7 mm to 3.1 mm in increasing order. The lowest and highest positions are shown in Fig. 3.2; positions lower than 0.7 mm didn't touch the actuator for it has an initial curvature remaining from the manufacturing process <sup>18)</sup>. This initial curvature varies between experiments, so the cathode position is taken in relation to the fixed referential in Fig. 2.3.

For comparison, an experiment is performed in the traditional configuration

found in the literature, with anode and cathode both fixed against the IPMC in a cantilever configuration and without mechanical constraints, the input signal consisting of a sine wave of  $\pm 3$  V in 30 Hz.

The time recorded was of 5 s before and 85 s after the input was being applied. All measured quantities were observed with the same oscilloscope with a sampling rate of 1 ms.

0s	Out of water, wipe water
60s	Apply $\pm 3$ V 0.5 Hz sine wave
80s	Apply 0 V
90s	Move cathode, observe touching point
140s	Apply DC 3 V
230s	Apply 0 V, back up cathode
260s	Apply $\pm 3$ V 0.5 Hz sine wave
280s	Apply 0 V
290s	Back in water

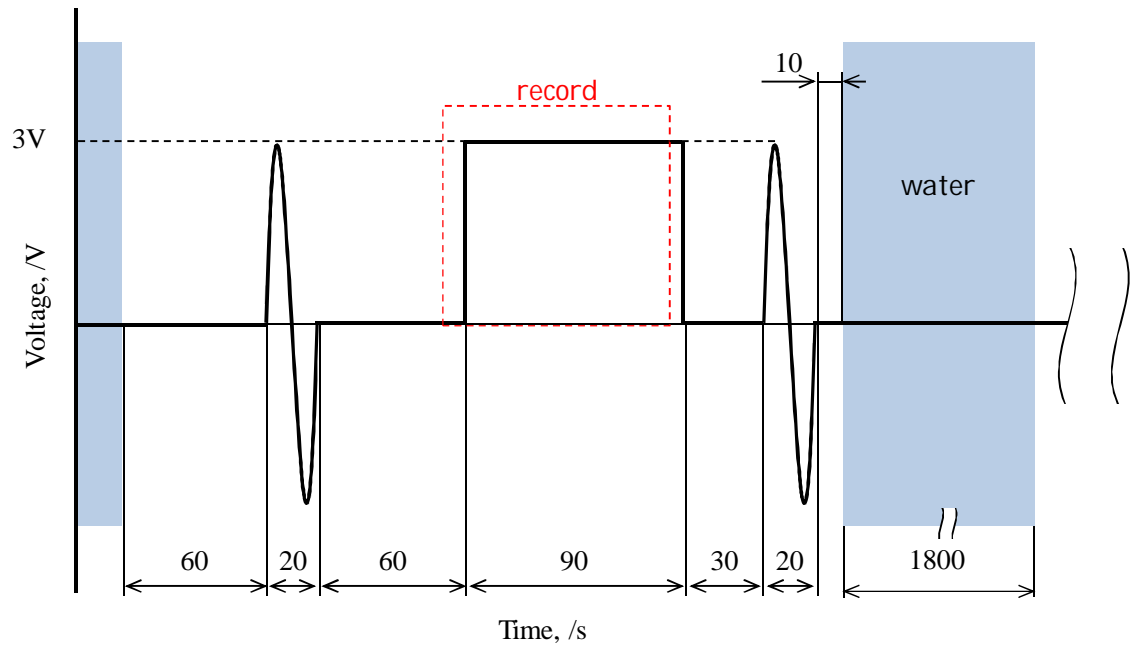
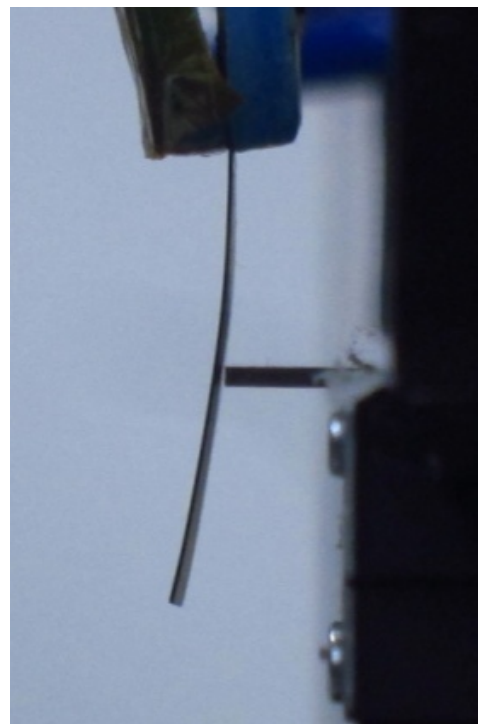


Fig. 3.1 Experimental timing



(a) 0.7mm



(b) 3.1mm

Fig. 3.2 Close up on the lowest and highest initial cathode positions

### 3.3 Results and discussion

The entire recorded results are shown in order of the absolute cathode position, followed by the sine wave experiment in Fig. 3.3. The lack of repeatability has been one of the biggest challenges throughout this research. Choosing environmental conditions and cathode material as explained in the previous chapter has made oscillations possible. However, as seen in the results in Fig. 3.3, long-term oscillations in air, even under traditional alternating voltages, are still erratic mainly due to the dehydration of the actuator and the lack of repeatability still persists to an extent. Nevertheless, some trends could be observed and will be discussed in this section, starting from the initial response, which was remarkably influenced by the cathode position.

#### 3.3.1 Initial response analysis

A close up on the first 0.2 s of oscillation for each experiment is shown in Fig. 3.4. As earlier described, when the input is switched on, the actuator receives an impulse while it is touching both electrodes. During the *first impulse*, the tip displacement increases as in a usual step response. Eventually, the actuator loses contact with the cathode, ending the first impulse, and the voltage read across it shows the value which has been charged onto the actuator.

The terms which will be used in this characterization are defined in Fig. 3.5. The *duration of the first impulse* ( $\Delta t_i$ ) is the time the actuator takes to lose electrical connection with the cathode for the first time since the input is turned on. The impulse duration is calculated as follows.

$$\Delta t_i = t_{if} - t_{is} + s \quad (3.1)$$

Here,  $t_{is}$  is the impulse start time,  $t_{if}$  the impulse final time, and  $s$  is the sampling rate of the results (1 ms). The separation position is taken to be the tip displacement at  $t_{if}$ .

In Fig. 3.6 the duration of the first impulse and the separation position are plotted for each cathode position. The further the IPMC is pushed, the longer it takes to separate from the cathode at first. The duration of the first impulse agrees well with the cathode position measured in relation to a fixed referential, suggesting that the initial curvature of the actuator does not influence this quantity.

Up to the moment of separation, the input is a simple 3V step. The displacement curves for all cathode positions taken from the moment the input is turned on follow the same path very closely. The first separation position in relation to the duration of the first impulse is plotted in Fig. 3.7 for all positions. This curve suggests that all experiments responded with the same tip displacement path, differing only by the time in which the step was turned off (contact lost).

Electrical and mechanical properties of IPMCs are independent <sup>9)</sup>. That is, for different initial deflections mechanically forced, as in this case, the actuator will exert the same force when under the same voltage. From classical beam theory it is understood that force and deflection are directly proportional; this could be the reason why despite different cathode positions, tip displacements follow closely the same path up to separation.

The exact condition for separation is not well understood yet. Typical IPMC cantilevers bend unevenly and their curvature distribution is related to the fixed end and to the position of the powering electrodes <sup>18)</sup>. In this case the powering electrodes are found at different positions and there is an additional mechanical constraint, giving rise to a complicated bending yet to be analyzed in depth.

After the IPMC separates from the cathode, it gains momentum to overshoot and elastically return stumbling onto the cathode once more. When it returns elastically, it doesn't press far enough to return to the original zero and quickly gets another impulse and separates quicker than the first time. This gives an impression that the origin has been shifted, but what happens is that the IPMC's curvature is not able to return to its initial value before separating again.

The *origin shift* defined in Fig. 3.5 (a) is taken to be the difference between the

lowest position reached when the beam returns ( $r_2$ ) and the initial origin ( $r_1$ ),  $r_n$  standing for the trough of the  $n$ th wave (likewise,  $c_n$  stands for the  $n$ th crest). The origin shift is plotted according to the initial cathode position in Fig. 3.8. These two quantities are related in a way that the further the cathode position, the larger distance the origin will be shifted, and the further away from the initial position the actuator will oscillate.

The origin shift is almost indistinguishable from the separation position at first, but they were defined as two different quantities since the origin shift varies throughout the oscillation as visible in the troughs of oscillation in Fig. 3.3.

### 3.3.2 Oscillation analysis

As described earlier, the actuator's tip overshoots when it receives an impulse and separates from the cathode, returning elastically and receiving a following impulse. For less pressed cathode positions, after a few impulses the actuator stops stumbling into the cathode and vibrates viscoelastically away from it. The vibration is damped and the actuator eventually returns to the cathode starting another cycle. These oscillations will be referred to as *cyclic oscillations* and are defined in Fig. 3.9.

At times the consecutive impulses in a cycle go on stumbling on the cathode indefinitely, resulting in what will be called *continuous oscillations*. These oscillations are defined in Fig. 3.10.

The types of oscillation observed for each cathode position are summarized in Table 3.1 for each experiment. For cathode positions up to 1.1 mm, only cyclic oscillations are observed in the duration of the experiment. For positions from 1.3 mm to 1.7 mm, oscillations start cyclic, eventually transition to continuous and stay this way until the end of the experiment. Finally, for positions above 1.9 mm, the oscillations are continuous since the beginning of the experiment. This suggests that the type of oscillation is related to the cathode position. The more pressed, the less chances of the actuator vibrating viscoelastically in a bent position without touching the cathode.

### 3.3.2.1 Cyclic oscillation

As shown in Fig 3.9, the order of a cycle during cyclic oscillations will be referred to as  $k$ , the order of an impulse inside a cycle as  $n$  and the total number of impulses in a cycle as  $m$ . The displacement waves will be numbered with the same notation as their respective impulses.

#### Return

The main characteristic of cyclic oscillations is that the actuator stops receiving consecutive impulses at some point and takes time to return to the cathode.

As said earlier, IPMCs behave as capacitors. While the actuator is in contact with both electrodes, it is being charged, and when contact is lost, the circuit is open and the charge is stored. In its wet state, an IPMC does not hold charge efficiently however <sup>10)</sup>, and quick leakage is observed during separation. When leakage is not as fast as charging, the actuator eventually reaches voltage saturation, as happened for cathode position 1.3 mm in Fig 3.3 (d).

Since the deformation of IPMCs is directly related to the applied voltage, the tip displacement should return along the leaking voltage. However, in the case of metallic ions, there's another returning mechanism which works during non-alternating inputs as explained previously, called back-relaxation.

To demonstrate the way a charged IPMC works in an open circuit, two quick experiments are performed. In the first one 3 V are applied to the actuator for 20 s and then the IPMC is shorted; in the second one, the specimen is charged the same way for 20 s and then the circuit is opened. The results are shown in Fig. 3.11. It's visible that when the circuit was opened, even though quick leakage happened at first, the displacement decay which was already happening due to back relaxation wasn't significantly affected.

This shows that in cyclic oscillations the main reason for the actuator's return is not electrical like in traditional mechanisms, but due to the back relaxation

which happens because of the return of water molecules.

### Cyclic frequency

A cycle will be defined electrically as a set of consecutive impulses and mechanically as the oscillations resulting from these impulses until the beam receives a new impulse. The period of a cycle is defined as follows.

$$C_p = t_{sn}^{k+1} - t_{sn}^k \quad (3.2)$$

Where  $t_{sn}^k$  stands for the *start time* of the  $n$ th impulse in the  $k$ th cycle. The cyclic frequency  $f_{cy}$  was taken as the inverse of the cycle period for each cycle and plotted against time in Fig. 3.12. For all cathode positions, the cyclic frequency increases with time. For the positions which didn't transition into continuous oscillation (0.7mm to 1.1mm), the frequency increases slower than for the ones which transitioned (1.3mm to 1.7mm). This suggests that there's a threshold position from where cyclic frequency accelerates until becoming continuous.

### Unforced frequency

Inside each cycle, there are viscoelastic vibrations which result from the transient impulse. These vibrations make the actuator stumble onto the cathode and receive further impulses which counter the damping in the vibration. When the actuator stops stumbling, the subsequent damped oscillations will be referred to as *unforced oscillations*. The frequency of unforced oscillations will be defined as the inverse of the average time between crest  $m$  and peak  $m+4$ .

$$f_u = \left( \frac{t_{cm+4}^k - t_{pm}^k}{4} \right)^{-1} \quad (3.3)$$

Unforced frequency  $f_u$  along time for different cathode positions is shown in Fig. 3.13. For all positions, the unforced frequency increased with time and stayed

between 29 Hz and 33 Hz. It is known that the actuator's stiffness increases with decreasing hydration<sup>5)</sup>, this is possibly the reason for the increase in frequency over time as water is evaporating.

Some difference in unforced frequency according to cathode positions is also visible but no immediate correlation with cathode position can be made. It's important to remember that the IPMC wasn't removed from the clip between experiments, and therefore the free beam vibrating is considered to be mechanically the same. It's also important to remember that the beam here is in a constrained configuration, which gives rise to complicated vibration modes.

### Effective voltage

After the first impulse, when the actuator touches the cathode again, even with leakage, typically there's still residual voltage across it. The difference between the *impulse's average voltage*  $V_{\text{avg}}$  and the *impulse starting voltage*  $V_{\text{is}}$  will be referred to as the *effective voltage*  $V_e$  as defined in Fig. 3.5 (b).

Fig. 3.14 relating the first amplitude ( $a_1^k = c_1^k - r_1^k$ ) in a cycle to the first effective voltage suggests these quantities are proportional. These results also suggest that their relation is the same independently of the cathode position, which can be explained by the independency of mechanical and electrical phenomena in IPMCs which has been previously mentioned: independent of the initially induced deformation, for a same effective voltage a same amplitude will be achieved.

It is noticeable that the effective voltages for the first impulse ( $k=1$ ) don't follow the same trend as the rest. These voltages are high since the actuator starts discharged. The first amplitude, unlike all the following ones, includes the origin shift plus the elastic overshoot. The present results don't present a strong correlation between amplitude and effective voltage for the first cycle in an oscillation.

## Amplitude

The p-p amplitude during cyclic oscillations varies inside a cycle as well as between cycles. Due to water loss, the oscillation along time for each experiment shows little consistency. Nevertheless, these experimental results suggest some characteristics regarding p-p amplitude.

*Amplitude change* will be defined as:

$$\Delta a = \frac{a_n^k}{a_{n-1}^k} \quad (3.4)$$

The average of the amplitude change for each crest order  $n$  for all cathode positions is shown in Fig. 3.15. For all cathode positions, the second impulse significantly increases the amplitude of oscillation, and higher order impulses tend to maintain the same amplitude as before.

As previously explained, the first amplitude in a cycle ( $n=1$ ) depends on the effective voltage. In Fig. 3.16 (a), the total number of impulses in a cycle ( $m$ ) is shown according to the average of the first amplitude in that cycle. Except for the cathode position 0.7 mm, this relation suggests that the lower the first amplitude is the more impulses are received until a cycle ends.

*Cycle amplitude ratio* will be defined as:

$$a_r = \frac{a_m^k}{a_1^k} \quad (3.5)$$

This number is shown in Fig. 3.16 (b) and shows how much the first amplitude increases until vibration stops stumbling onto the cathode. The higher the number of impulses, the higher is the difference between the last and first forced amplitudes.

### 3.3.2.2 Continuous oscillation

## Frequency

It was decided that a maximum of 3 consecutive troughs without impulses will be tolerated as part of a continuous oscillation as shown in Fig. 3.10 (a). The

continuous frequency was calculated as:

$$f_{co} = \left( \frac{t_{co5} - t_{col}}{4} \right)^{-1} \quad (3.6)$$

Where  $t_{col}$  and  $t_{co5}$  are the times of crests in the middle of the oscillation which are 5 crests apart, taken every 2 s as shown in Fig. 3.10 (b). The continuous oscillation frequency along time for different cathode positions is shown in Fig. 3.17.

For all cathode positions which presented continuous oscillation the frequency increases with time. However, some results are accelerating while others seem to move towards a steady frequency during the observed time.

For those positions which transitioned from cyclic to continuous oscillation, it's interesting to notice that the continuous frequency starts slightly higher than the unforced frequency which happened during the cyclic oscillation.

The continuous oscillations for the 3.1 mm cathode position stopped for about 30 s between time 32 s and time 62 s. It is interesting to notice however that when the continuous oscillations restarted, the frequency seems to continue accelerating in the previous trend, suggesting that the frequency acceleration is not related to the continuity of the oscillation itself, but to time and dehydration.

The same way as for the unforced frequency, the frequency here is thought to increase due to dehydration and increased stiffness. Since voltage is applied more often here, the actuator loses water quicker than during cyclic oscillations.

For some results, 1.9 mm (Fig. 3.3 (g)) for example, the effective voltage remains steady throughout the experiment, which suggests that the charging and leakage of the IPMC are in equilibrium. Yet, the frequency increases due to water evaporation. So it seems safe to assume that under conditions of controlled hydration, steady prolonged oscillation could be achieved using the novel approach introduced here.

### Peak-to-peak amplitude

Continuous oscillations happen when every elastic vibration of the beam

stumbles onto the cathode and receives a new impulse as if there was an infinite cycle. As explained before about amplitude of cyclic oscillation, higher order impulses in a cycle tend to counter damping and maintain the amplitude of oscillation stable in relation to the previous impulse. Indeed, in continuous oscillations, the p-p amplitude at small periods of time is so stable that they look like undamped elastic vibrations.

Changes in p-p amplitude for continuous oscillations come gradually, and as shown in Fig. 3.18, continuous p-p amplitude decreases with time. The effective voltage throughout continuous oscillations is quite steady, which suggests that the decay in p-p amplitude is due to the loss of water molecules and decreased pumping effect.

#### Peak-to-peak amplitude and frequency

The relation between p-p amplitude and frequency for continuous oscillations is shown in Fig. 3.19. There's a clear relation between frequency and p-p amplitude for each cathode position. It is thought that due to the transient elastic nature of these oscillations, the actuator is always oscillating at its natural frequency, so this graph could be showing how the resonant peak of the actuator changes for different levels of hydration.

#### 3.3.3 Comparison with a traditional sine input

The same way as the DC input results, the tip displacement for the 30 Hz sine input seen in Fig. 3.3 (n) is unsteady, having varying amplitude and origin during the observed time. Due to the nature of the input, the movement's frequency is steady.

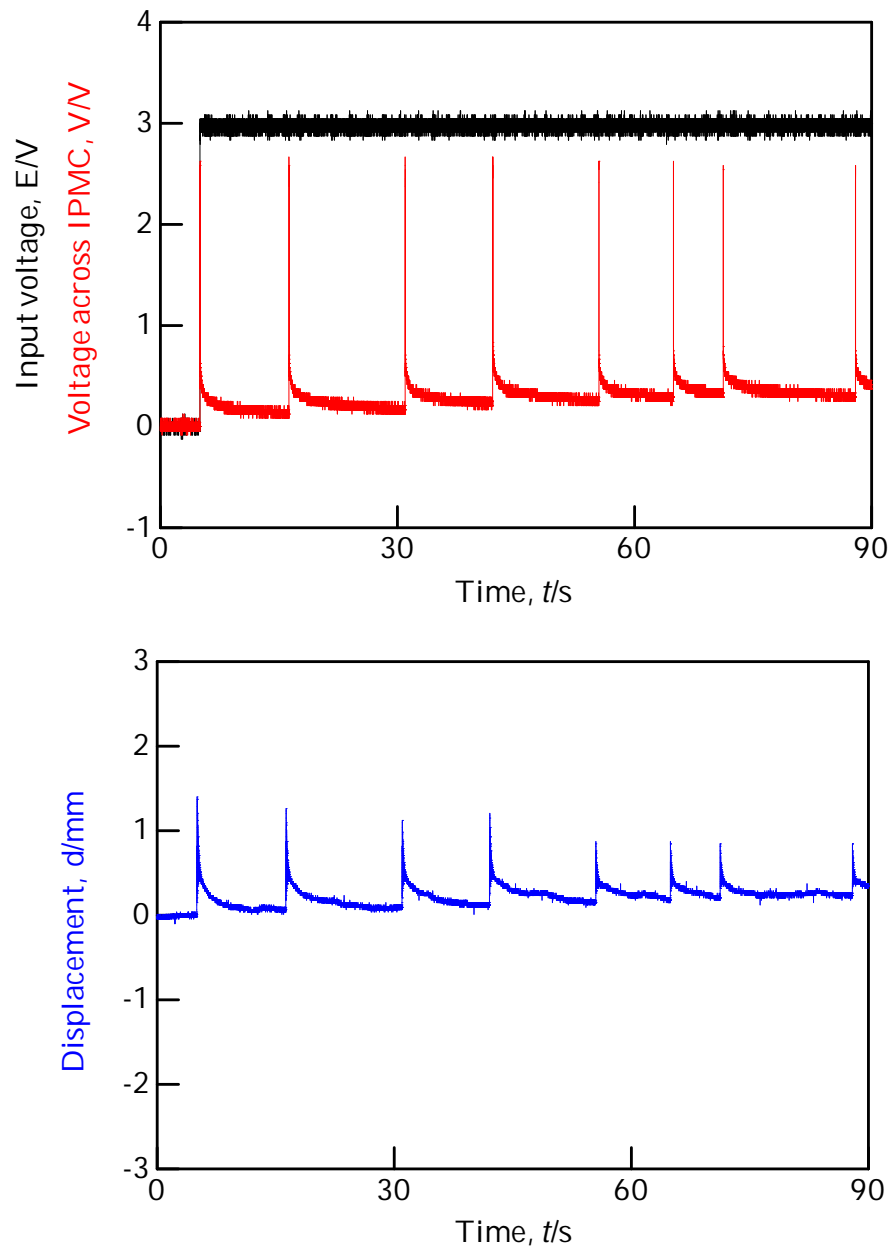
The maximum amplitude achieved at the beginning of the oscillation reached 6 mm but soon after decayed below 1 mm, having a second peak of 3.4 mm and once more falling under 1 mm as seen in Fig. 3.18. This peak in amplitude could be explained as the moment that the resonant frequency of the drying actuator

reached 30 Hz for that momentary level of hydration. Another possible explanation is that the hydration of the specimen has reached about 70%, as shown in <sup>27)</sup>, which is when the number of water molecules is just right to be carried along the Na<sup>+</sup> ions without obstructing their way.

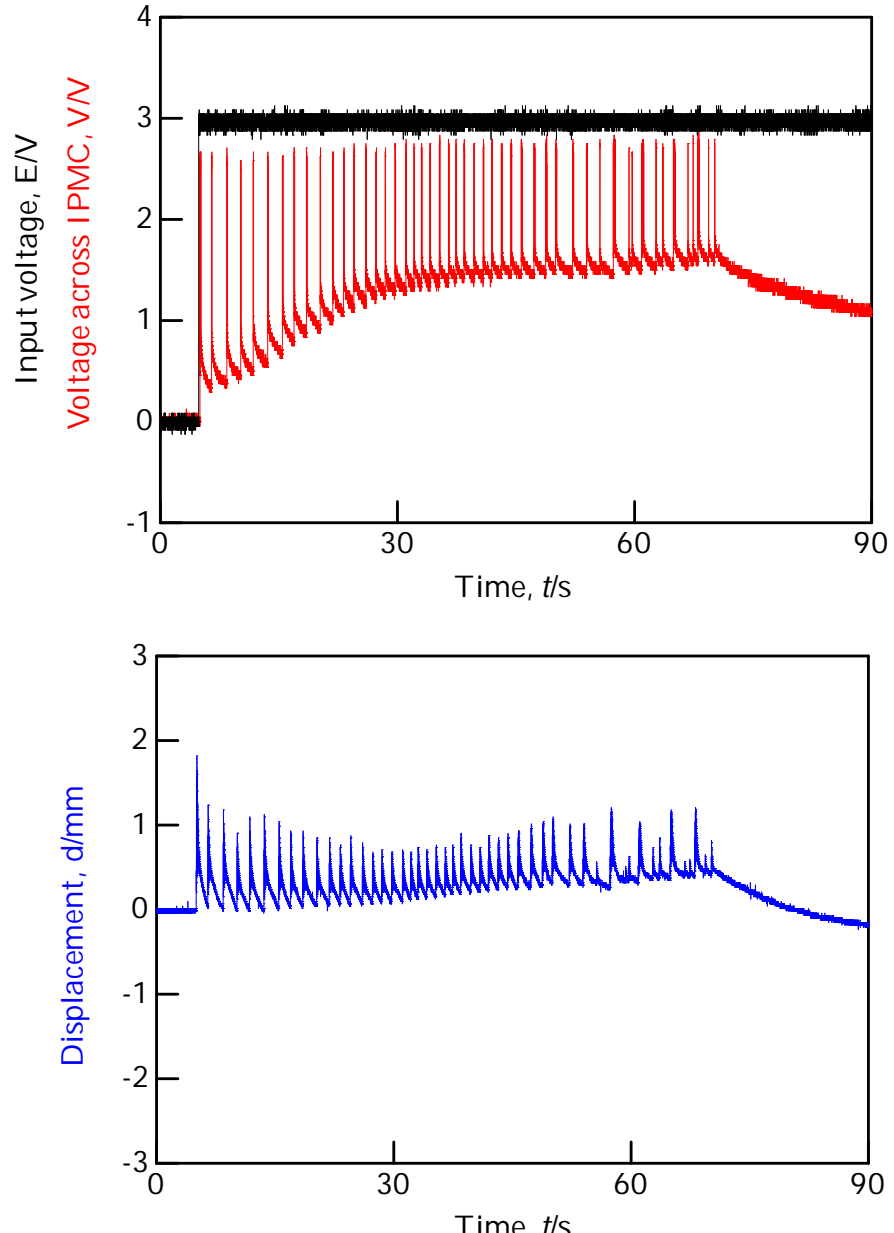
The main results for the cathode positions which were fully continuous and for the sine input are shown in Table 3.2. While the highest amplitude achieved with DC oscillation (2.167 mm) was only 36 % of that achieved with the sine input (6.083 mm), the highest average amplitude for the DC oscillation (1.14 mm) was 71 % of that achieved with the sine input (1.605 mm).

During traditional AC oscillations, ions are being electrically pulled at every stage. In DC oscillation however, elasticity and mobility of water molecules are the main mechanisms of oscillation, and still the amplitudes reached are in the same order as those of traditional systems, while consuming less power and simplifying electronics.

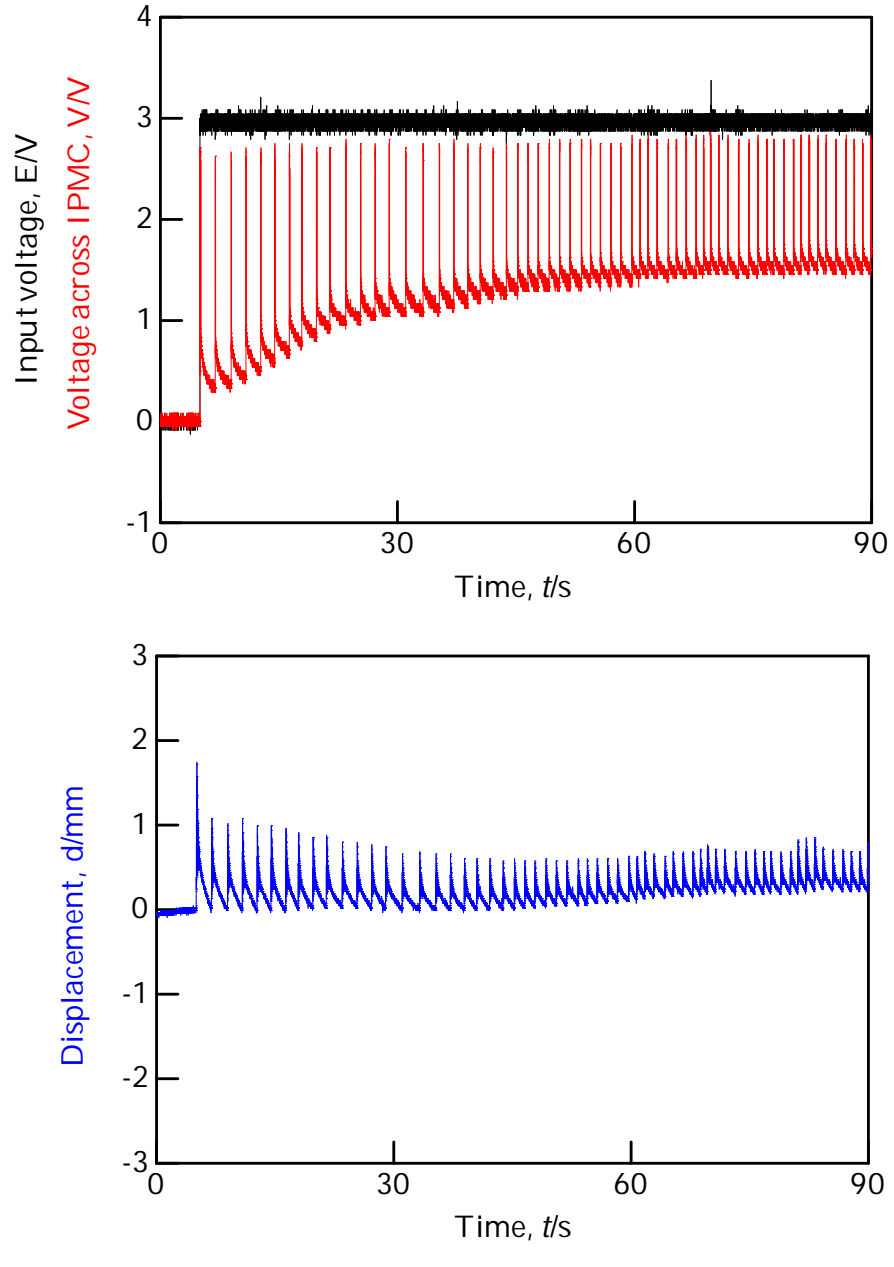
It is safe to assume however that the new system presented here does not exert forces comparable to traditional systems in both directions of oscillation. Moreover, they are less electronically controllable. Nevertheless, these results are very promising and introduce a new approach as a possible alternative to be used in systems which require less electronics and don't require high force outputs in both directions of oscillation.



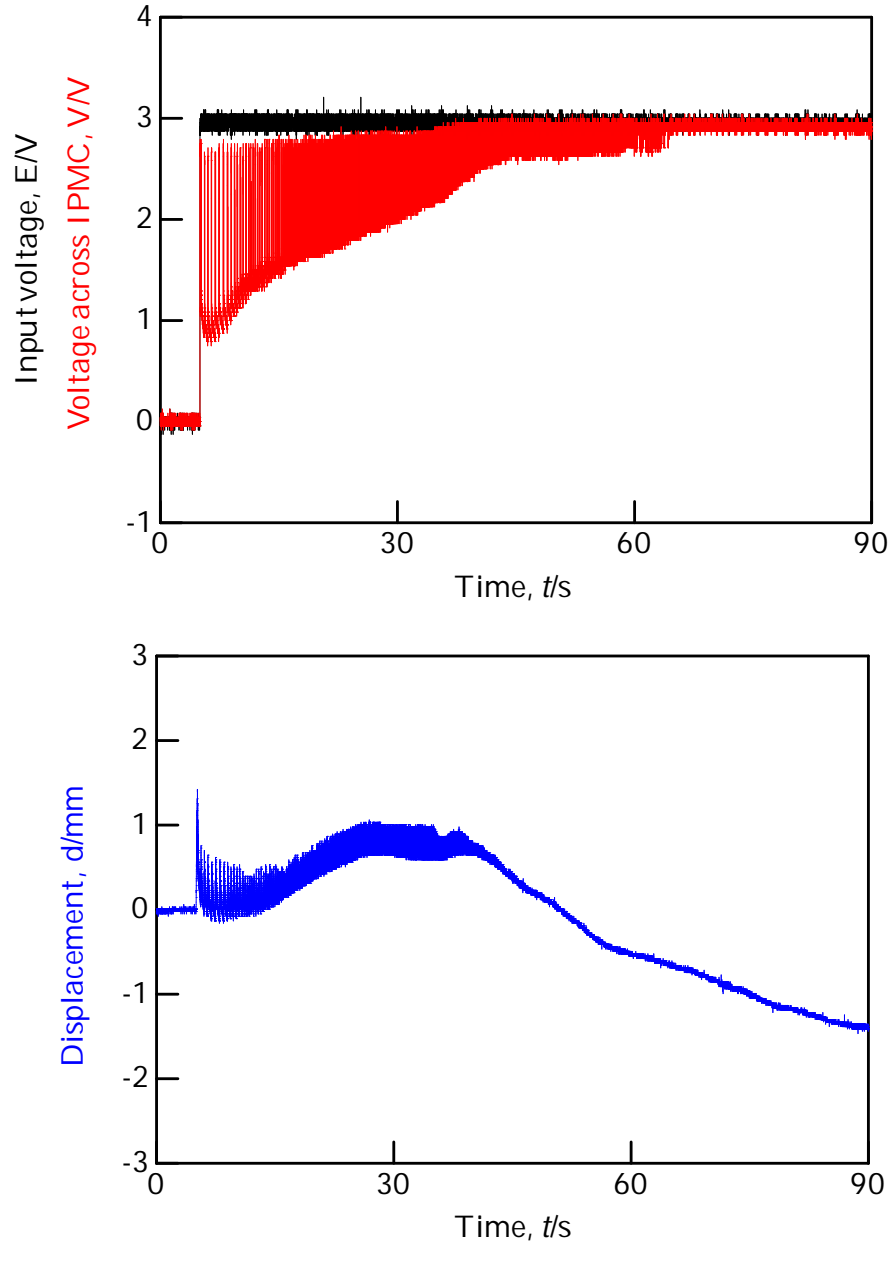
(a)  $x = 0.7$  mm



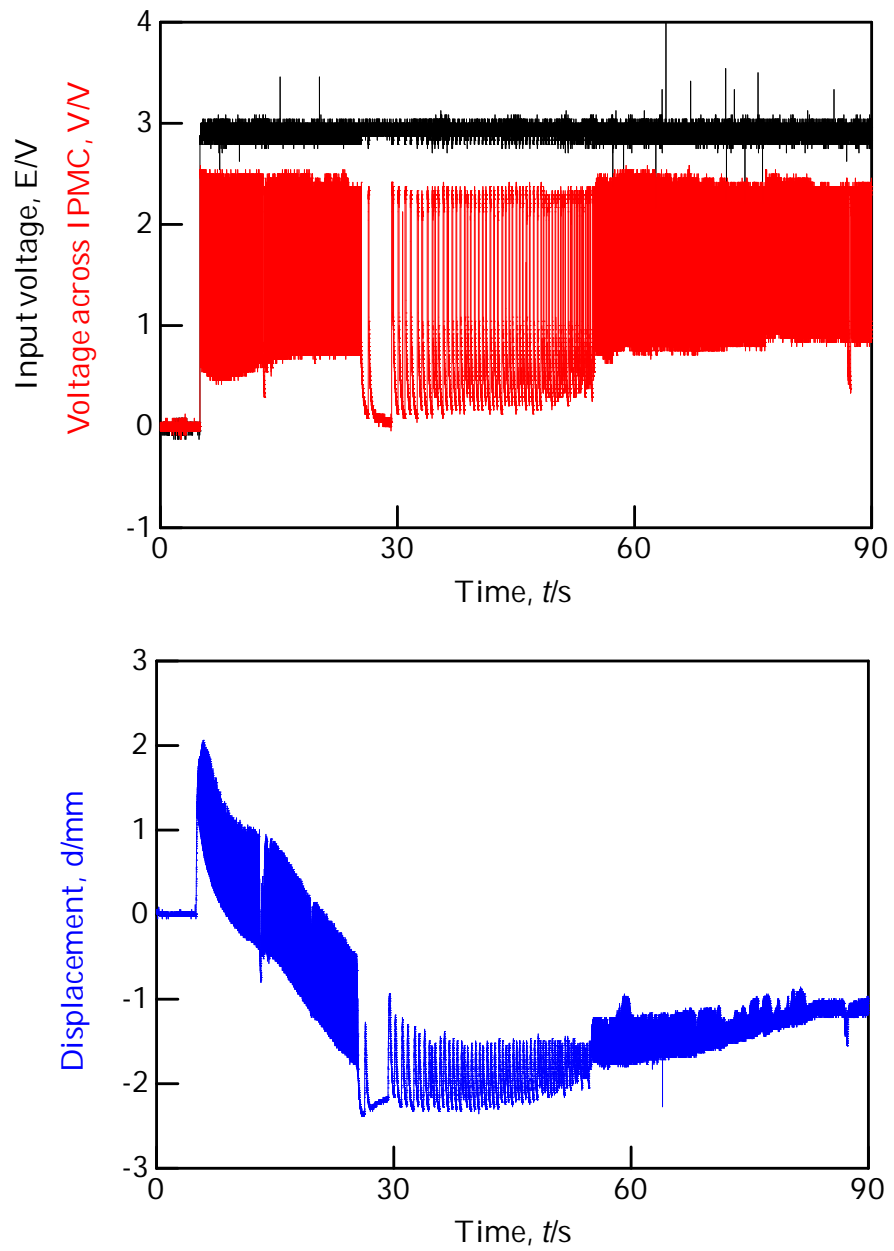
(b)  $x = 0.9$  mm



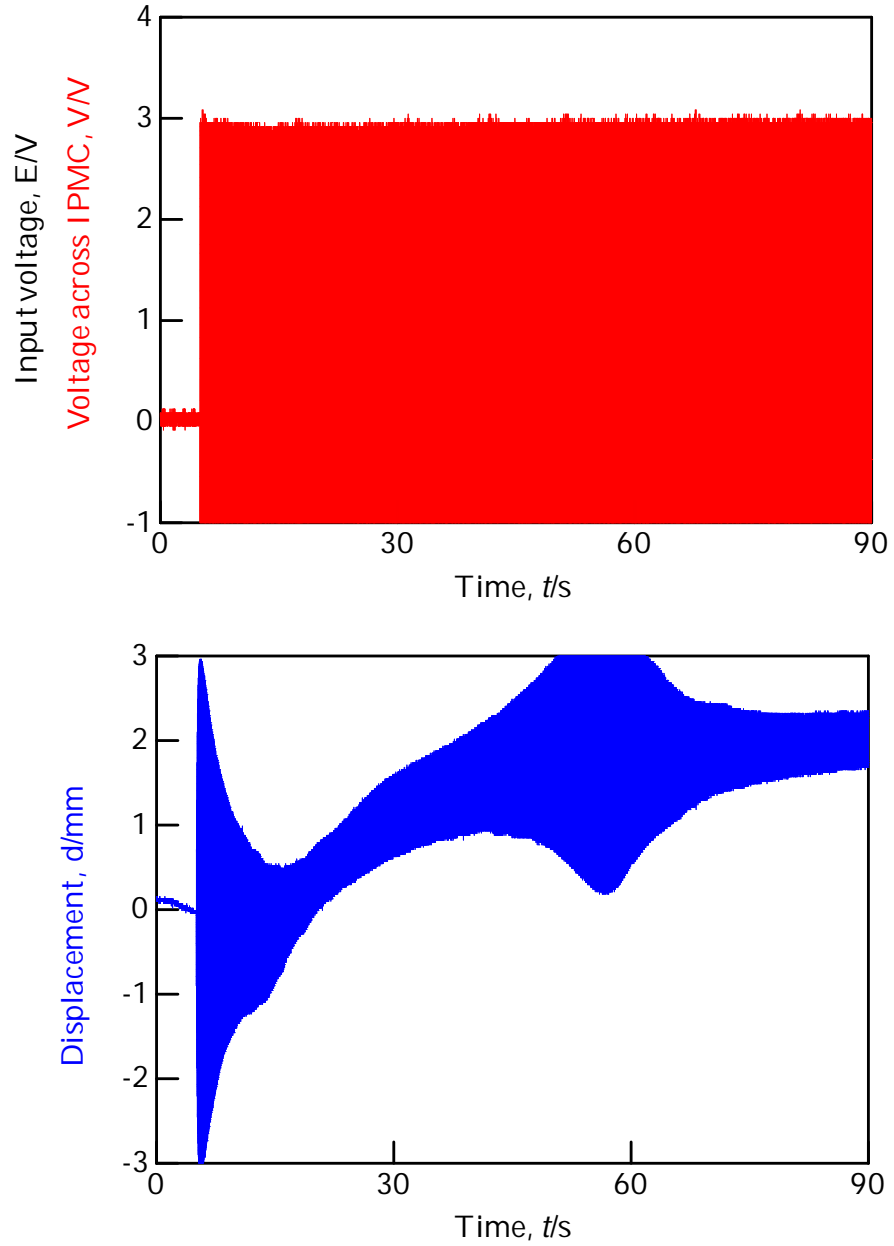
(c)  $x = 1.1$  mm



(d)  $x = 1.3$  mm

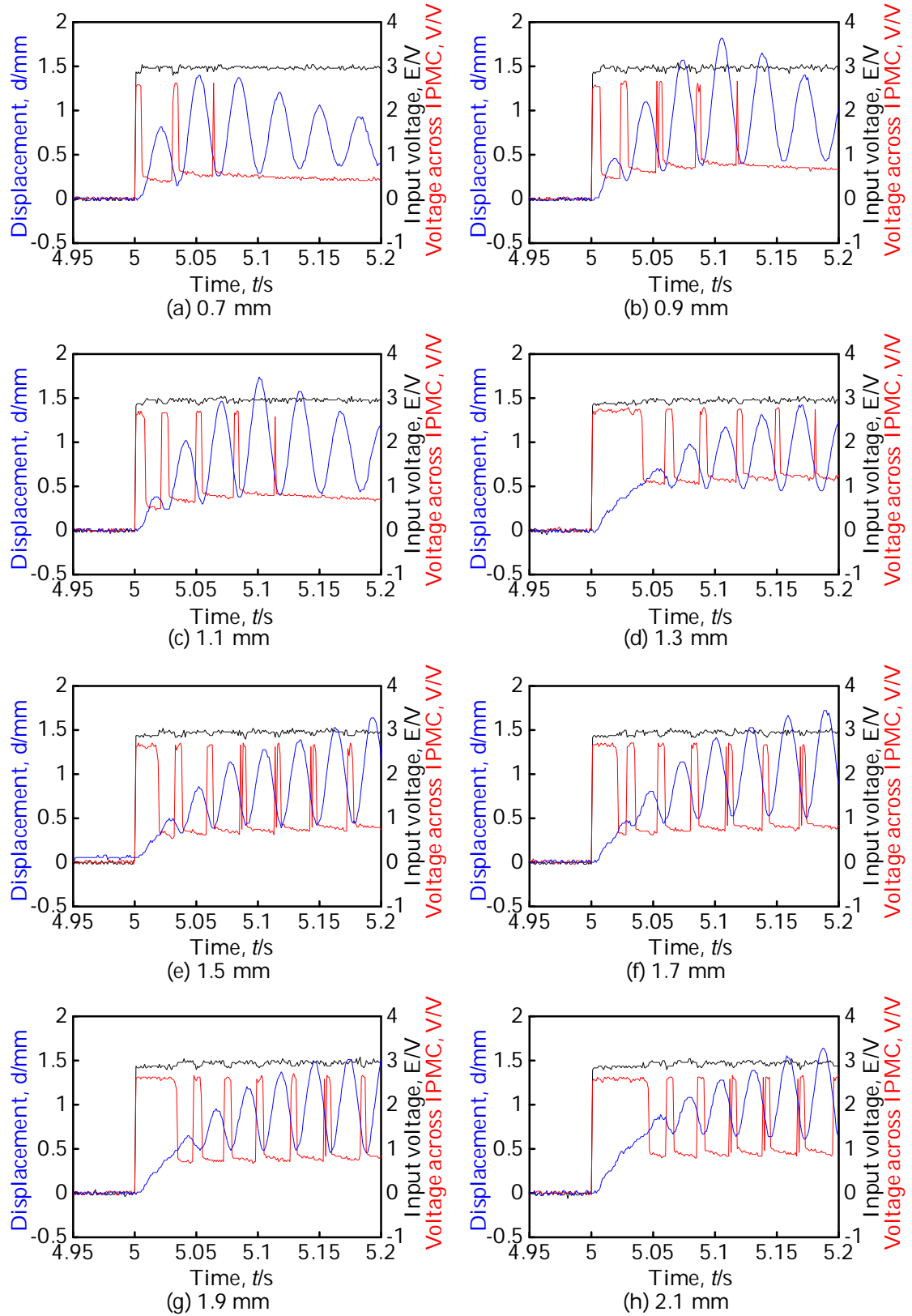


(m)  $x = 3.1 \text{ mm}$



(n) 30 Hz sine wave

Fig. 3.3 Oscillation for different cathode positions along the x axis and for a 30 Hz sine wave input



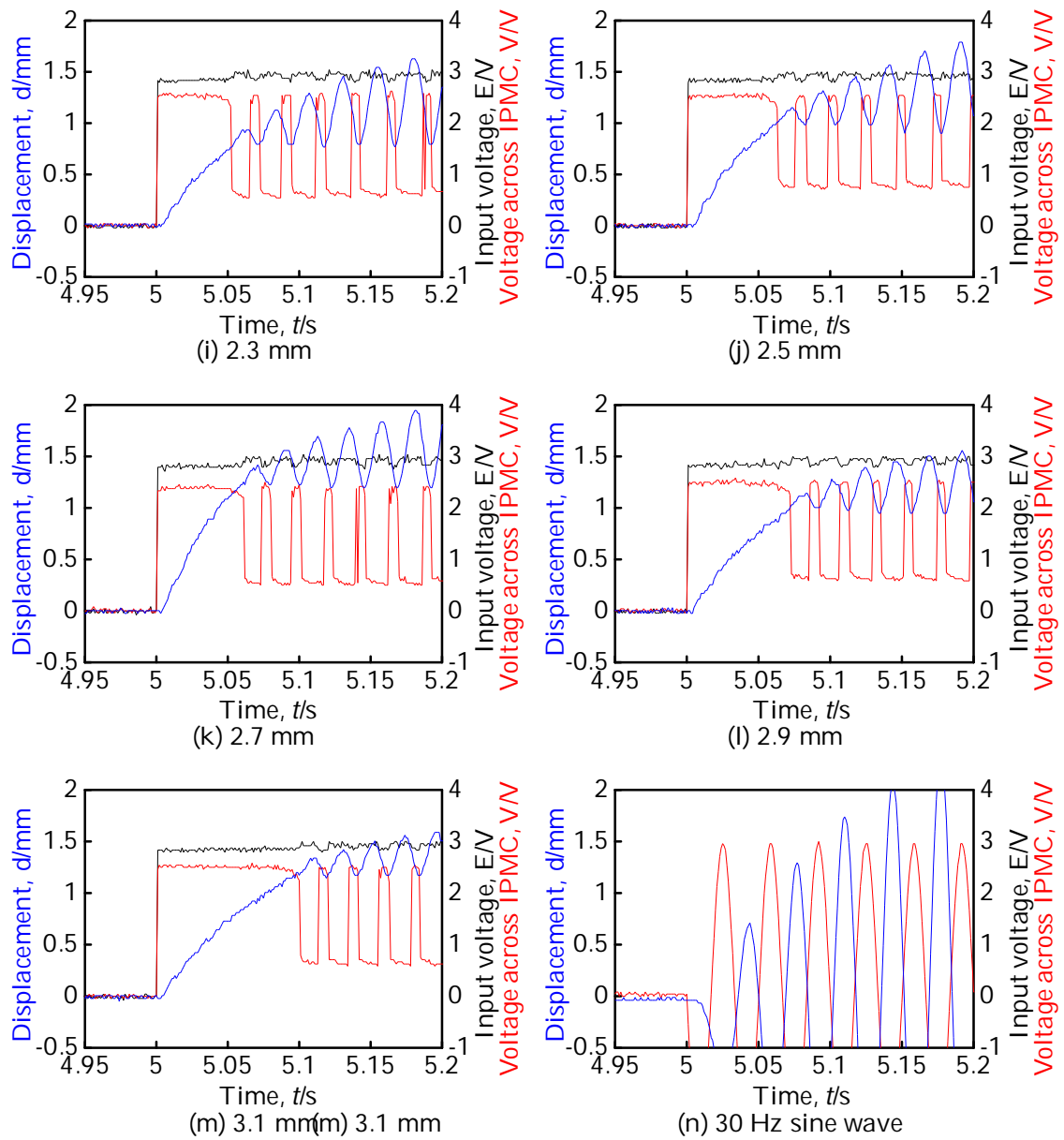
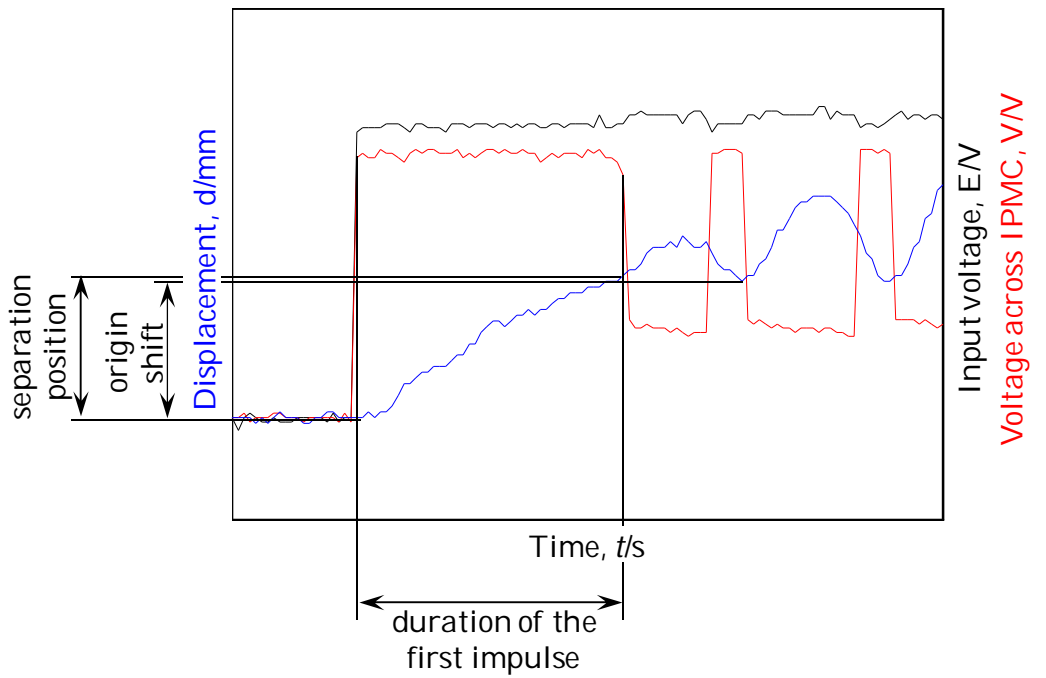


Fig. 3.4 Close up on the first 0.2 s of oscillation for each cathode position  
and for a 30 Hz sine wave input



(b) Initial response displacement definitions

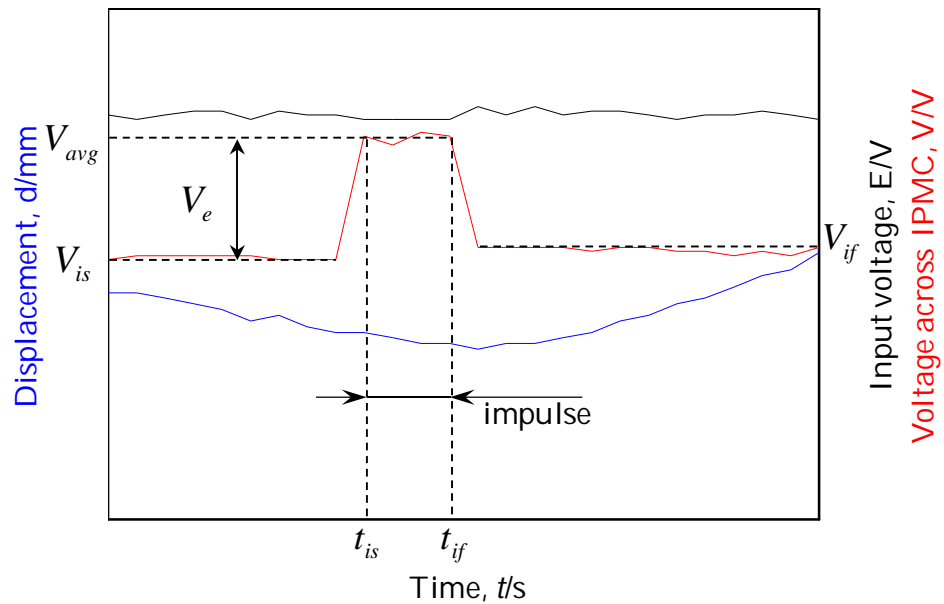
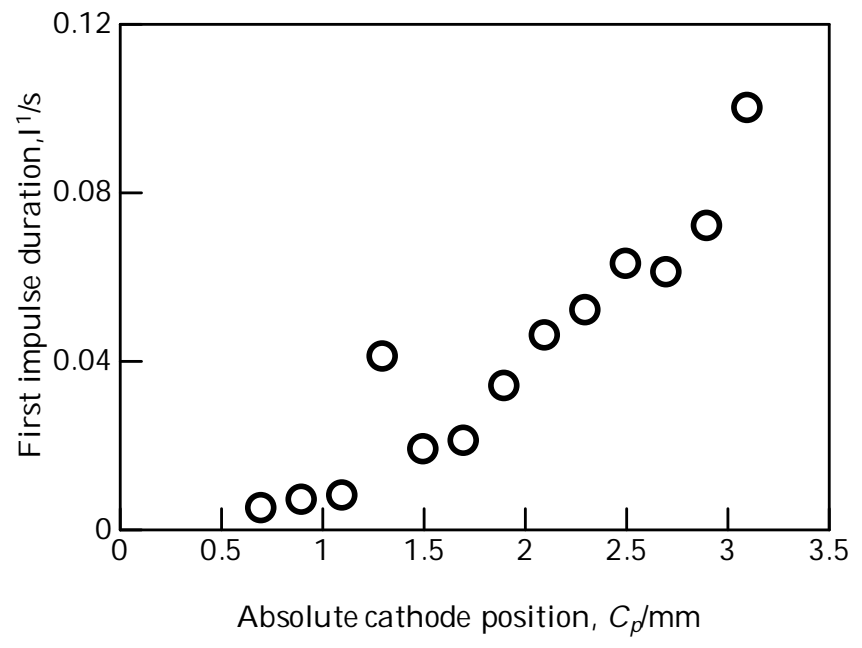
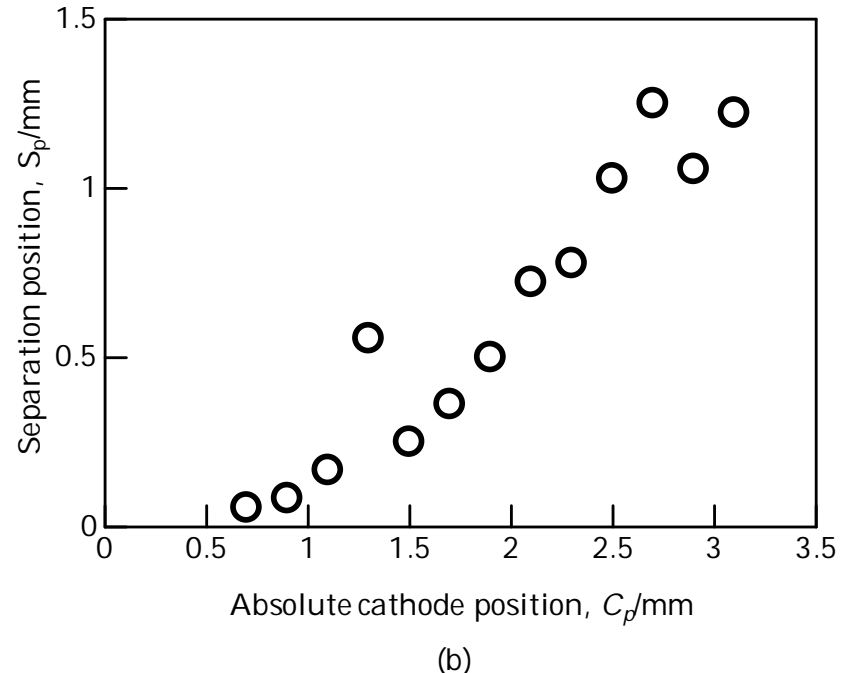


Fig. 3.5 Initial response definitions



(a)



(b)

Fig. 3.6 First impulse duration and separation position for each cathode position

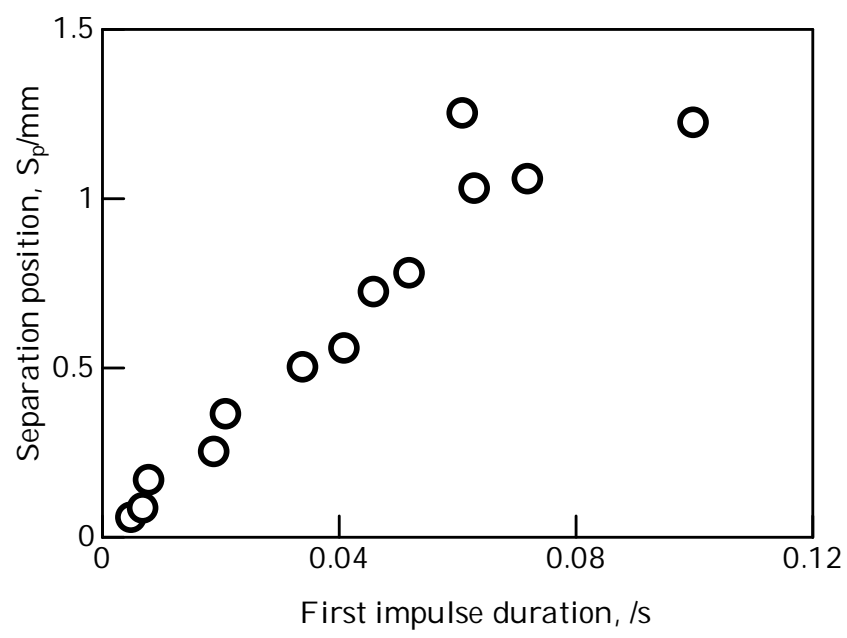


Fig. 3.7 Duration of the first impulse and its first separation position

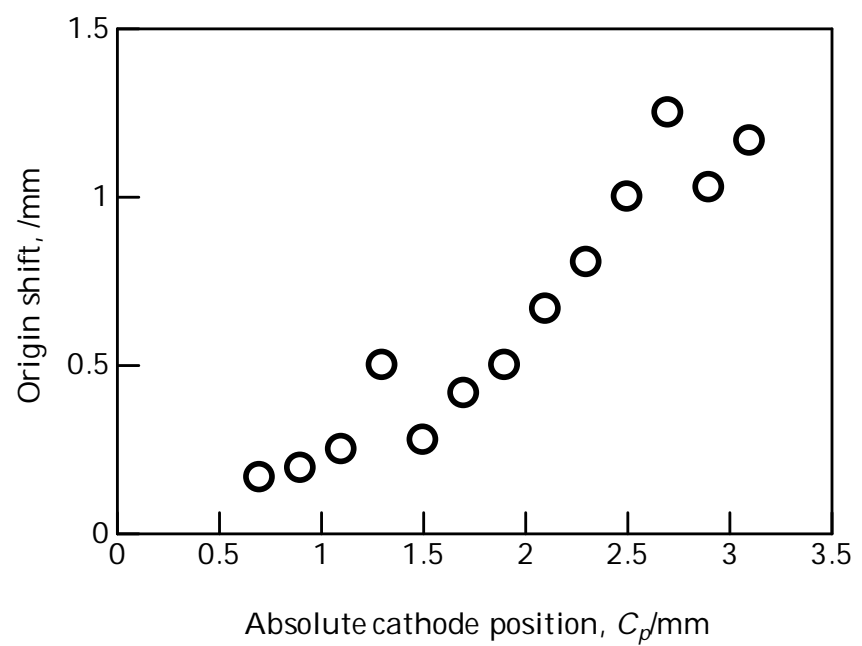
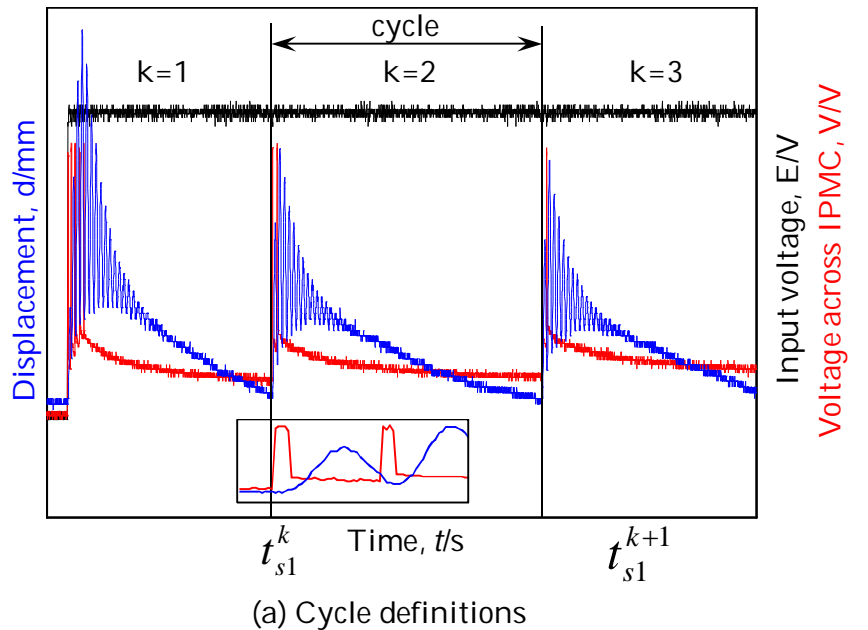


Fig. 3.8 Origin shift for different cathode positions



(a) Cycle definitions

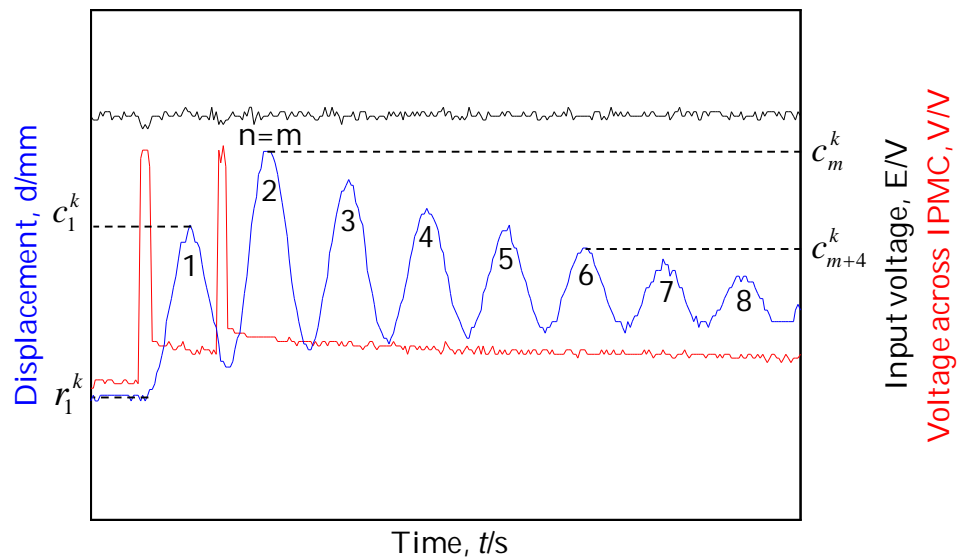
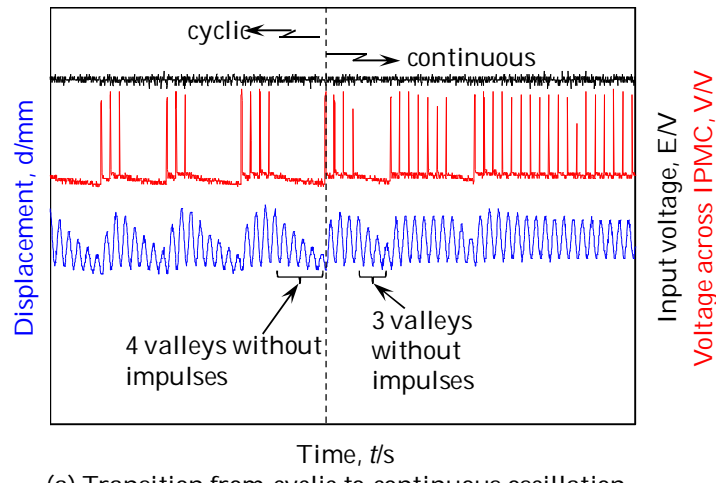
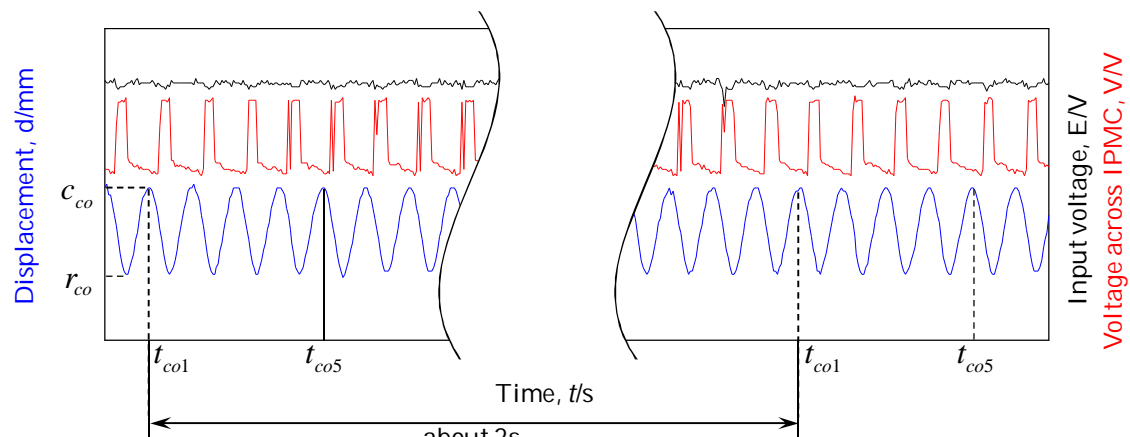


Fig. 3.9 Cyclic oscillation definitions



(a) Transition from cyclic to continuous oscillation



(b) Displacement definitions

Fig. 3.10 Continuous oscillations definitions

Table 3.1 Types of oscillation per cathode position

Cathode position (mm)	Representation	Cyclic oscillation	Continuous oscillation
0.7	○ black	✓	□
0.9	△ red	✓	□
1.1	□ blue	✓	□
1.3	○ lightgreen	✓	✓
1.5	△ orange	✓	✓
1.7	■ magenta	✓	✓
1.9	○ lightbrown	□	✓
2.1	△ brown	□	✓
2.3	□ purple	□	✓
2.5	▽ lightblue	□	✓
2.7	◇ gray	□	✓
2.9	○ dark pink	□	✓
3.1	★ dark green	□	✓
sine	✗ yellow		

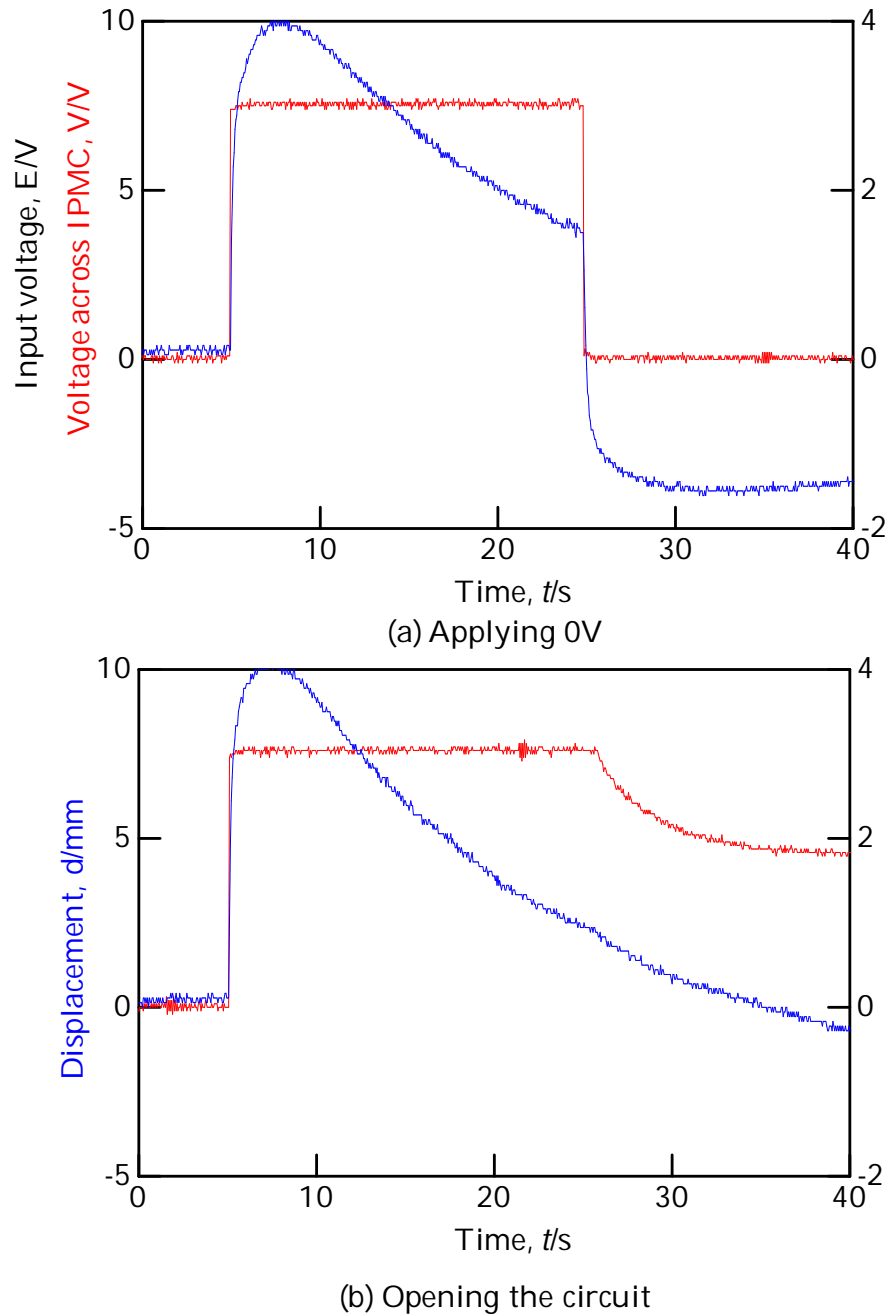


Fig. 3.11 Comparison between IPMC's return to the origin by applying 0V and by opening the circuit

Cathode position (mm)	Representation	Cyclic oscillation	Continuous oscillation
0.7	∅ black	✓	□
0.9	△ red	✓	□
1.1	□ blue	✓	□
1.3	● light green	✓	✓
1.5	▲ orange	✓	✓
1.7	■ magenta	✓	✓

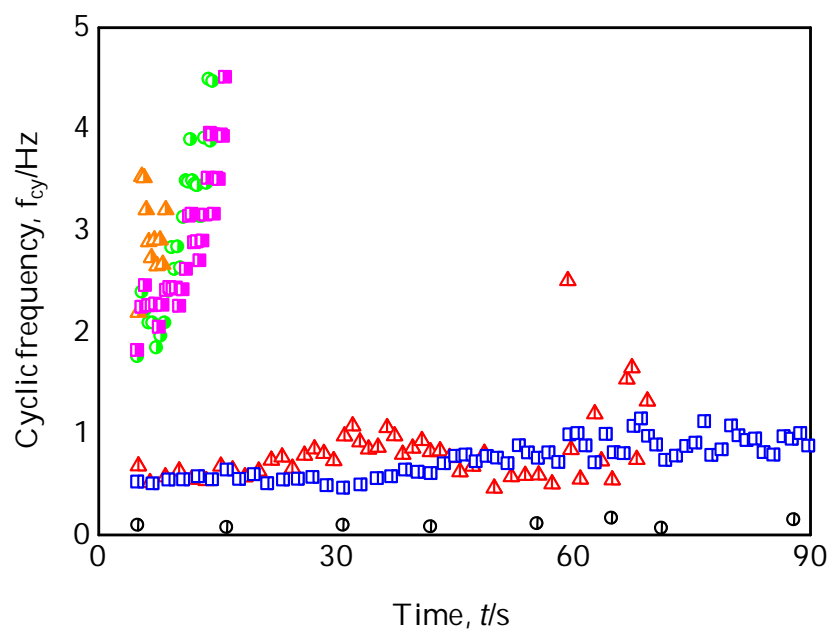


Fig. 3.12 Cyclic frequency along time for different cathode positions

Cathode position (mm)	Representation	Cyclic oscillation	Continuous oscillation
0.7	∅ black	✓	□
0.9	△ red	✓	□
1.1	□ blue	✓	□
1.3	● light green	✓	✓
1.5	▲ orange	✓	✓
1.7	■ magenta	✓	✓

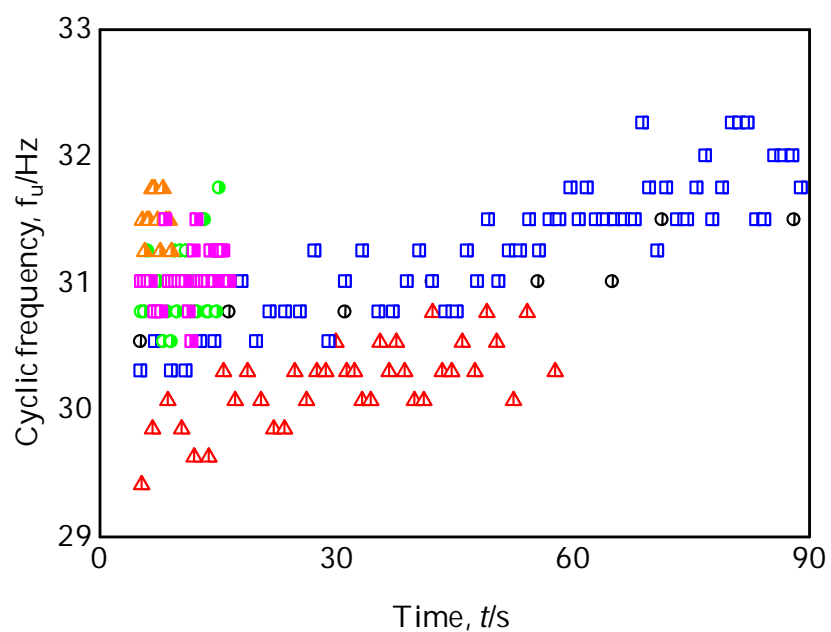


Fig. 3.13 Unforced frequency along time for different cathode positions

Cathode position (mm)	Representation	Cyclic oscillation	Continuous oscillation
0.7	∅ black	✓	□
0.9	△ red	✓	□
1.1	□ blue	✓	□
1.3	● lightgreen	✓	✓
1.5	▲ orange	✓	✓
1.7	■ magenta	✓	✓

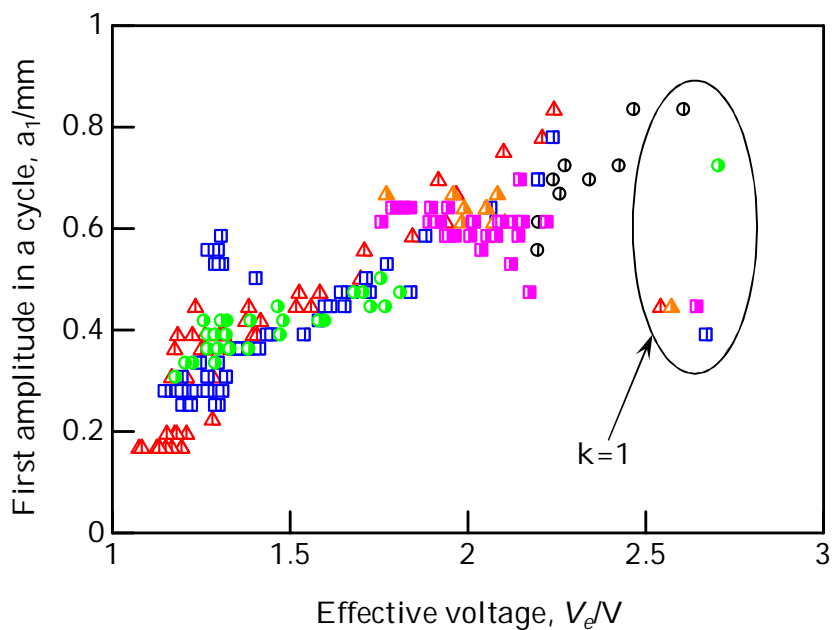


Fig. 3.14 First amplitude in a cycle in relation to the first effective voltage

Cathode position (mm)	Representation	Cyclic oscillation	Continuous oscillation
0.7	∅ black	✓	□
0.9	△ red	✓	□
1.1	■ blue	✓	□
1.3	● lightgreen	✓	✓
1.5	▲ orange	✓	✓
1.7	■ magenta	✓	✓

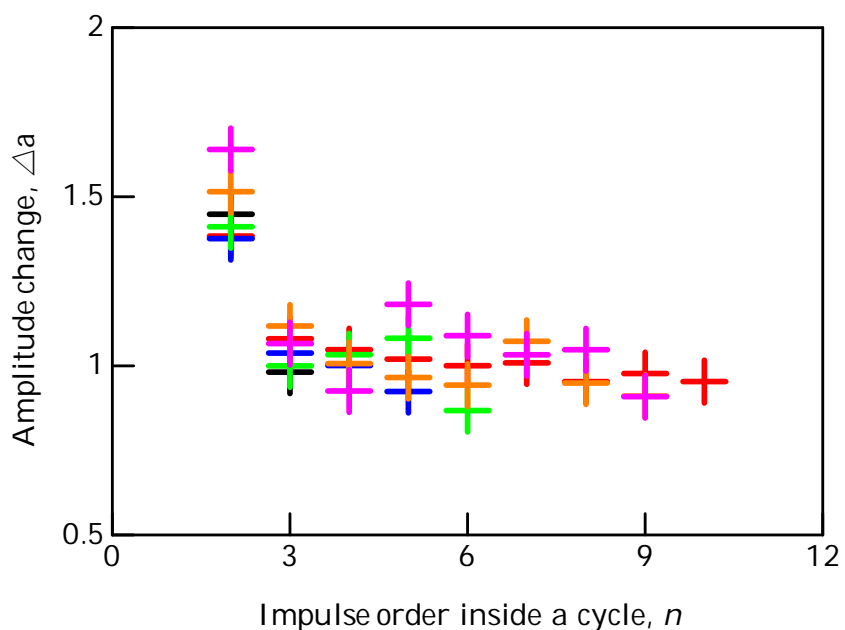
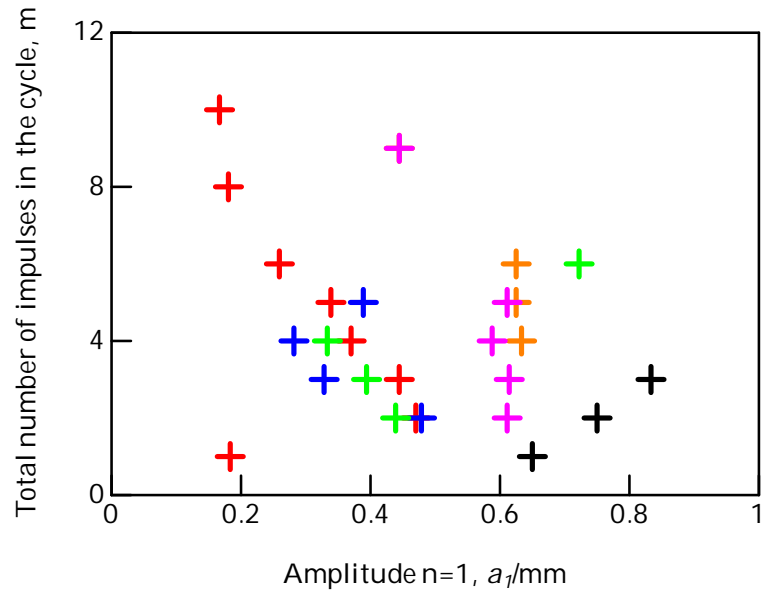
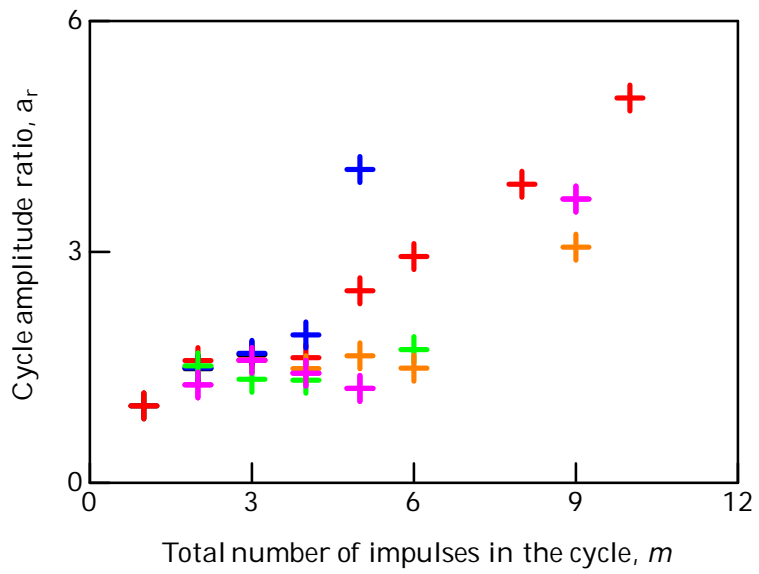


Fig. 3.15 Change in amplitude for the impulse order inside a cycle

Cathode position (mm)	Representation	Cyclic oscillation	Continuous oscillation
0.7	∅ black	☒	☐
0.9	△ red	☒	☐
1.1	□ blue	☒	☐
1.3	● light green	☒	☒
1.5	▲ orange	☒	☒
1.7	■ magenta	☒	☒



(a) According to the first amplitude



(b) According to the ratio between the last forced amplitude and the first amplitude

Fig. 3.16 Total number of impulses in a cycle

Cathode position (mm)	Representation	Cyclic oscillation	Continuous oscillation
1.3	○ light green	✓	✓
1.5	△ orange	✓	✓
1.7	□ magenta	✓	✓
1.9	○ light brown	□	✓
2.1	△ brown	□	✓
2.3	□ purple	□	✓
2.5	▽ lightblue	□	✓
2.7	◇ gray	□	✓
2.9	○ dark pink	□	✓
3.1	★ dark green	□	✓

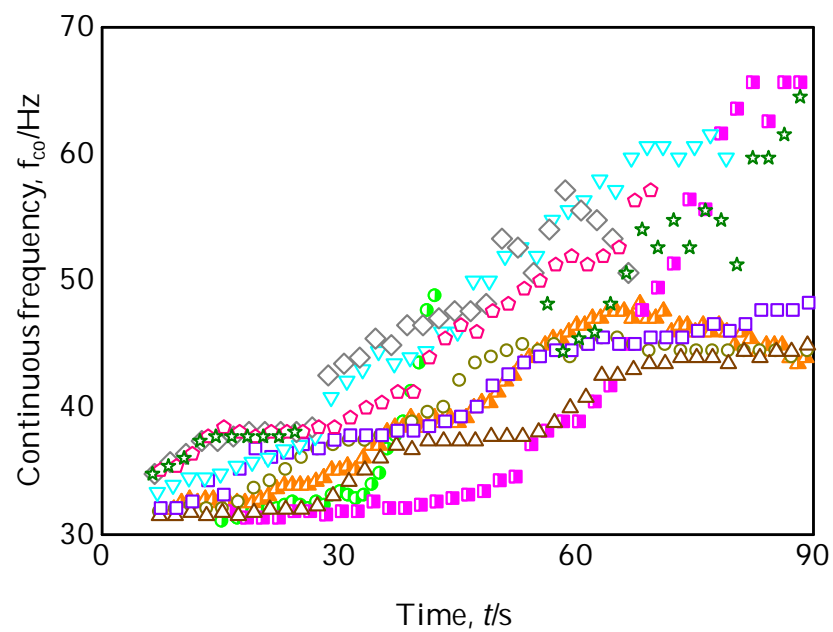


Fig. 3.17 Frequency of continuous oscillations along time for different cathode positions

Cathode position (mm)	Representation	Cyclic oscillation	Continuous oscillation
1.9	○ lightbrown	□	✓
2.1	△ brown	□	✓
2.3	□ purple	□	✓
2.5	▽ lightblue	□	✓
2.7	◇ gray	□	✓
2.9	◇ dark pink	□	✓
3.1	★ dark green	□	✓
sine	× yellow		

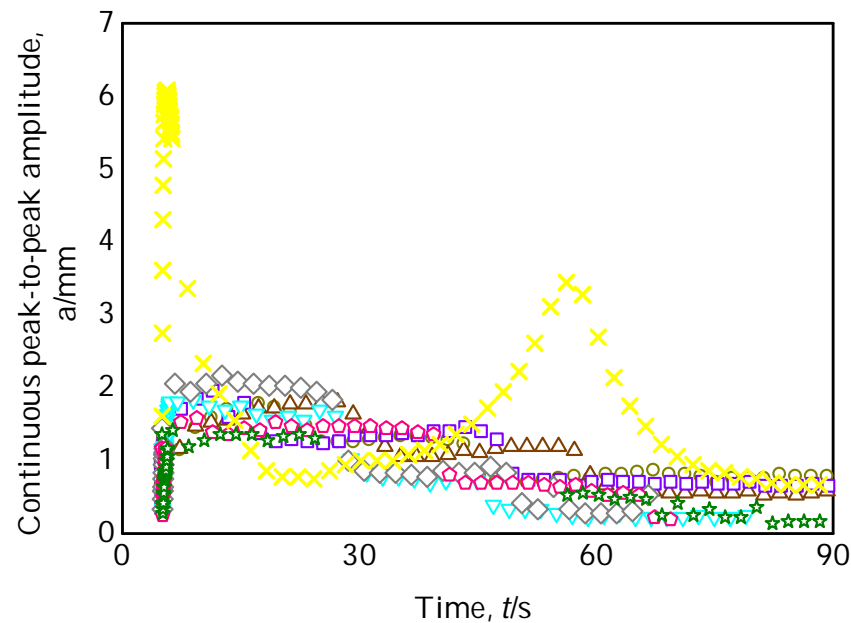


Fig. 3.18 Amplitude of continuous oscillations along time for different cathode positions

Cathode position (mm)	Representation	Cyclic oscillation	Continuous oscillation
1.3	○ lightgreen	✓	✓
1.5	▲ orange	✓	✓
1.7	■ magenta	✓	✓
1.9	○ lightbrown	□	✓
2.1	△ brown	□	✓
2.3	□ purple	□	✓
2.5	▽ lightblue	□	✓
2.7	◇ gray	□	✓
2.9	○ dark pink	□	✓
3.1	★ dark green	□	✓

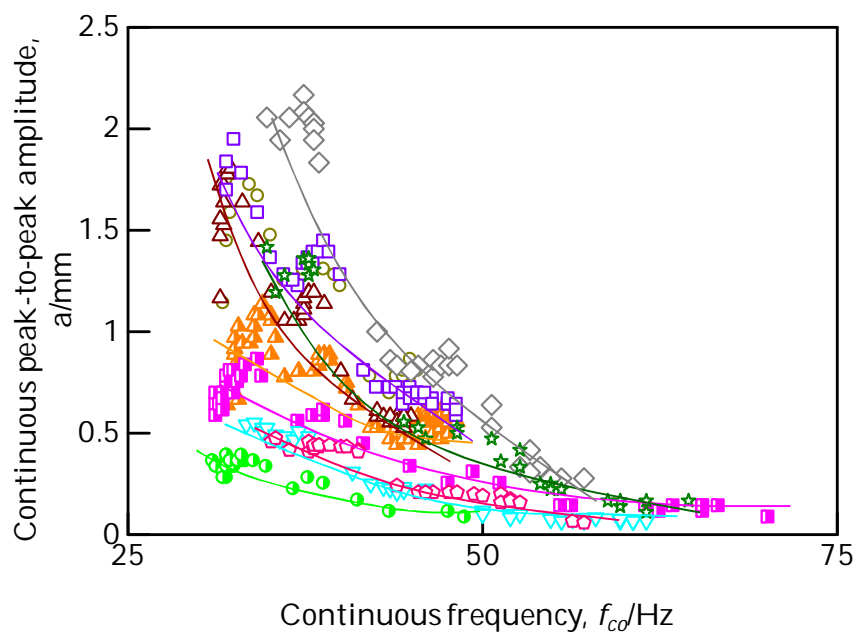


Fig. 3.19 Relation between peak-to-peak amplitude and frequency for continuous oscillations for different cathode positions

Table 3.2 Summary of main oscillation characteristics for positions fully continuous and for the sine input

Cathode position (mm)	Initial frequency (Hz)	Highest frequency (Hz)	Highest amplitude (mm)	Average amplitude (mm)
<b>1.9</b>	31.7	45.5	1.778	1.053
<b>2.1</b>	31.5	44.9	1.806	1.056
<b>2.3</b>	32.0	48.2	1.944	1.044
<b>2.5</b>	33.3	61.5	1.833	0.850
<b>2.7</b>	34.8	57.1	2.167	1.140
<b>2.9</b>	35.1	57.1	1.583	1.050
<b>3.1</b>	34.8	61.5	1.417	0.703
<b>sine</b>	30.0		6.083	1.605



## Chapter 4 Other Configurations

### 4.1 Introduction

This research has focused on a simple configuration in order to investigate the feasibility for obtaining oscillation making use of an IPMC's movement as a switch for the voltage applied across itself. The novel approach presented here is not limited to the presented configuration however. There's a wide range of possibilities not limited by the presently investigated shape of electrodes and actuators, type of input, mechanical constraints, etc.

### 4.2 Non-fixed pumping

The configuration shown in Fig. 4.1 consists of an IPMC with metal plates as extensions of one of its metal layers placed above an anode. When a voltage is applied between the base which the metal extensions touch and the anode in the center, the actuator bends downwards and eventually loses contact with the actuator. Contact is lost and no power is applied on the actuator, so it falls back onto the anode starting a new cycle. This configuration was attempted in air during this research and presented visible oscillations.

Unlike the experimented configuration, in this one the actuator is not fixed at all to the structure and is free to move along the anode's length.

### 4.3 Actuator between walls with a potential across them

The two configurations showed in Fig. 4.2 give the actuator the possibility of performing an oscillatory movement when between two walls which have an electric potential across them. Both in the case of a straight path or a bent path, the actuator can be shaped to bend in a way that it loses contact with one or both of the electrodes. Some researchers have succeeded in reshaping IPMC actuators with a simple heat treatment procedure <sup>16)</sup>.

This type of configuration was attempted in air and didn't present visible oscillations; after separation the actuator got stuck to the cathode wall due to the water in its surface. It is well known that during actuation, the cathode surface of this type of actuators gets relatively more hydrated to the point of water drops forming outside it <sup>5)</sup>, and this poses a challenge to the use of these configurations with this kind of actuators in air.

#### 4.4 Triple-snap

Snap-through of an IPMC has been achieved before by patterning its surface electrodes <sup>11)</sup> and by choosing well the shape of the actuator <sup>28)</sup>. A configuration which could provide good geometrical stability is shown in Fig. 4.3, where the actuator is fixed on both ends and compressed as a bilaterally constrained buckled beam <sup>29)</sup>. Anodes and cathodes would be alternately placed on the lateral walls in a way that two thirds of the IPMC are always inducing snap while only one third is resisting against it. This way there could be continuous bi-stable snap-through making use of a DC input.

#### 4.5 Free bender

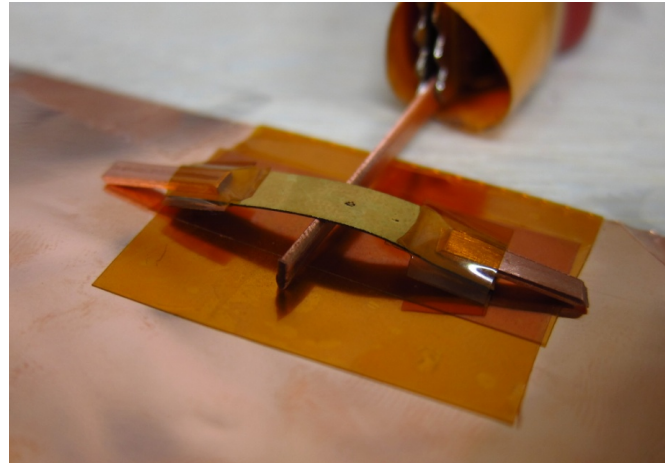
The great advantage of using transient interactions to obtain oscillation is the simplification of circuitry by using only a DC input, which can be provided by simple batteries. The concept in Fig. 4.4 puts together an IPMC and a thin-film polymeric battery <sup>30)</sup> as a self-contained smart oscillatory system. As the actuator bends towards the anode it loses contact with the battery's cathode turning power off and restarting a cycle. Since both elements are very thin and flexible, they could be combined in a variety of ways which use the IPMC's curvature as a switch and move freely.

#### 4.6 Bias structure

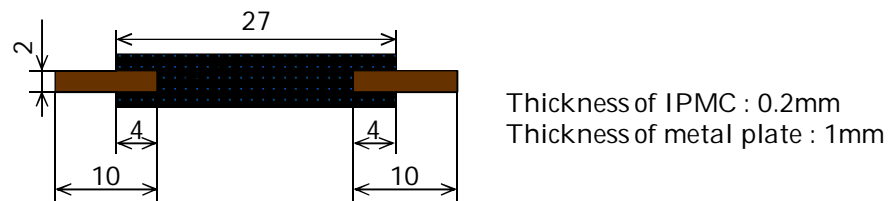
Another advantage of the present approach is the direct interaction with mechanical systems.

The spring bias structure in Fig. 4.5 (a) for example brings a membrane back to its place when it has been dislocated. A similar bias structure can be build using an IPMC as in Fig. 4.5 (b); the cathode would be placed so the IPMC gets actuated when the membrane is dislocated to a determined position and exerts a bias force to bring the membrane back. Without the need for extra sensors or processing, this system would work as a direct mechanical response to the position of the actuator.

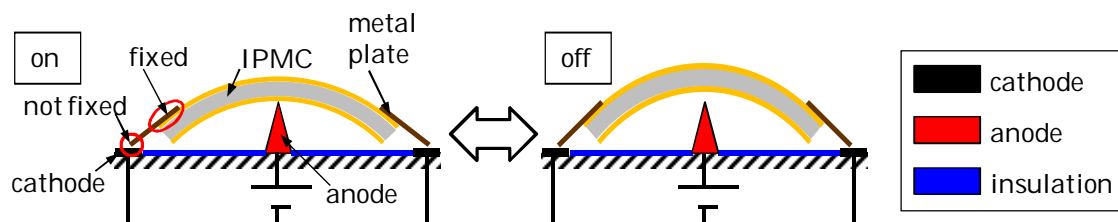
Unlike the spring structure, the IPMC structure exerts force in only one direction and only from a determined dislocation.



(a) Real appearance

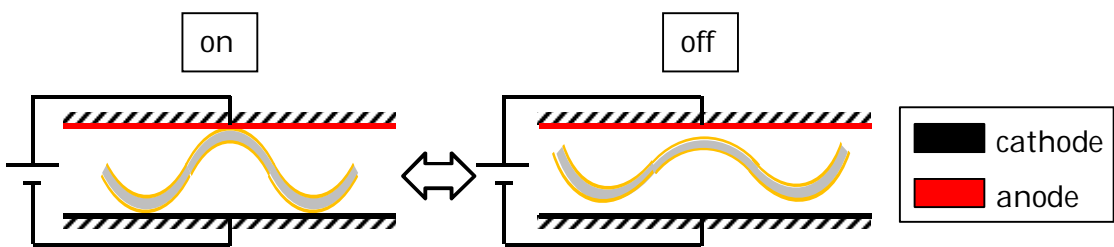


(b) Measures

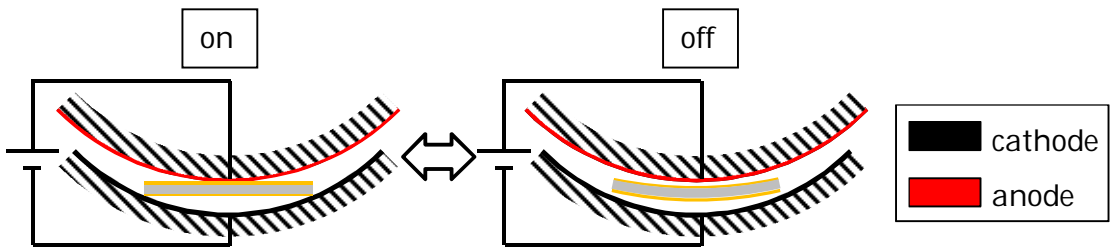


(b) Oscillation system

Fig. 4.1 Novel configuration: non-fixed pumping



(a) Curved IPMC in a straight path.



(b) Straight IPMC in a curved path.

Fig. 4.2 Novel configurations: actuator between walls with a potential across them

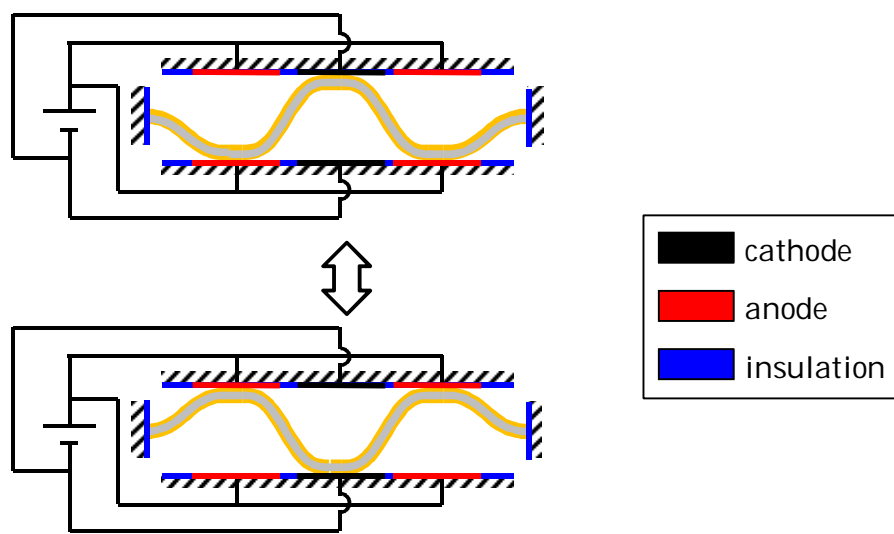


Fig. 4.3 Novel configuration: triple snap

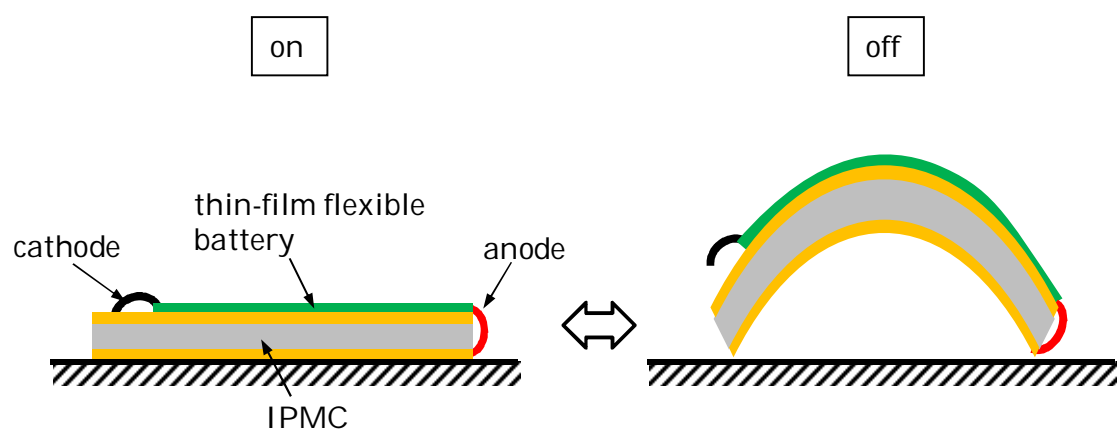


Fig. 4.4 Novel configuration: free bender

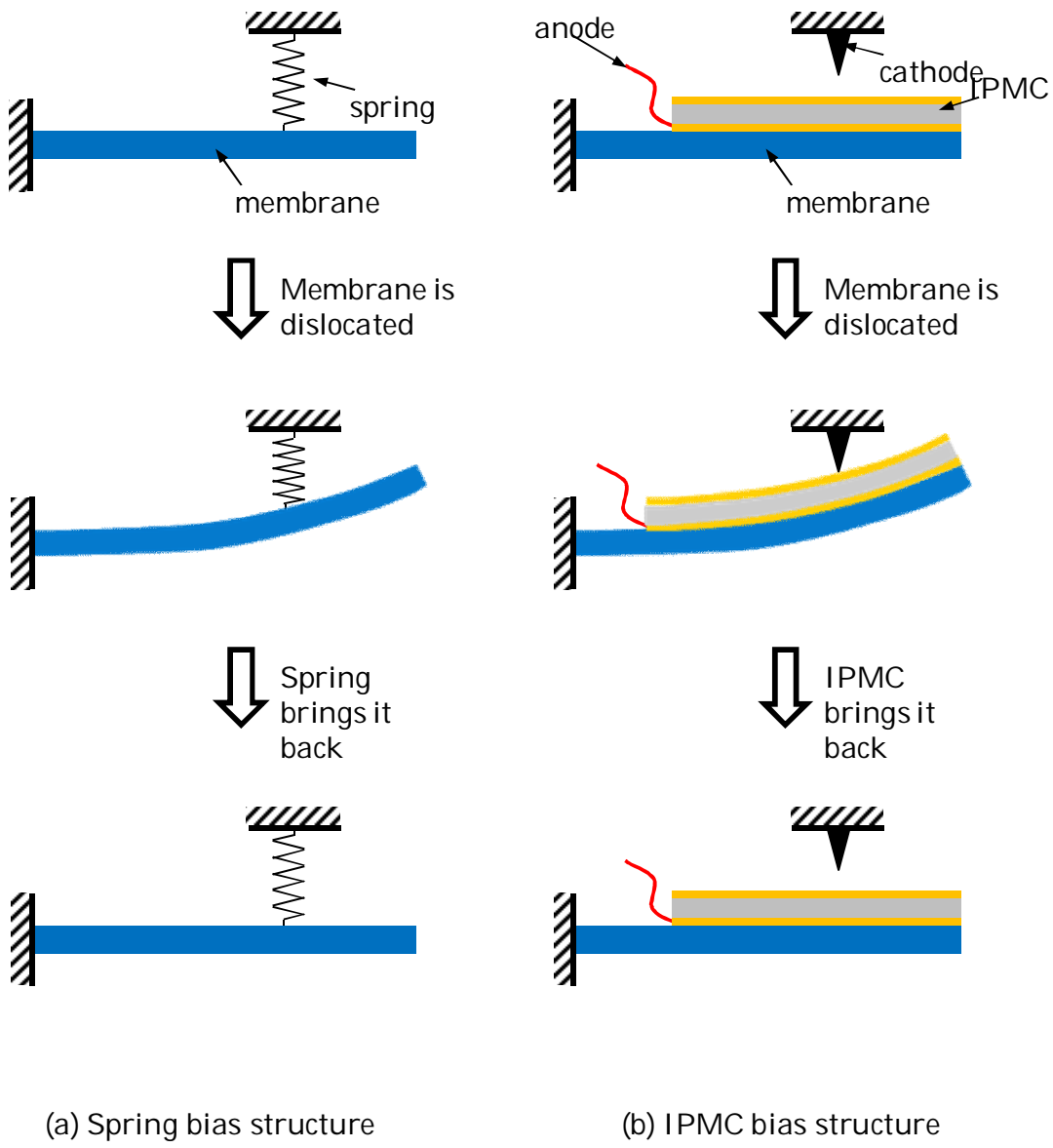


Fig. 4.5 Novel configuration: bias structure

## Chapter 5 Conclusions

In this paper, a new approach was introduced which uses a DC input to oscillate an IPMC actuator by making it lose contact with the electrodes which it gets power from.

The results were as follows:

- 1) For an actuator in a vertical cantilever configuration where it is fixed to the anode and can bend away from the cathode, oscillation was achieved.
- 2) Two materials were tested as the cathode, aluminum and copper. Copper was a more suitable material for the non-fixed electrode.
- 3) The cathode was pressed against the actuator at different positions along its orthogonal axis. Less pressed positions presented oscillation characterized by quick separations and slow returns in frequencies from 1.5 Hz to 5 Hz. More pressed positions presented uniform oscillations where the IPMC oscillates elastically and touches the cathode for a new impulse every cycle; these oscillations had frequencies between 30 Hz and 60 Hz.
- 4) In comparison with a traditional AC input, the newly proposed system had an average amplitude of over 70 % of that achieved with a sine input.

The newly proposed system require simple electronics and less wire connections having a big potential of substituting AC input systems in applications which don't require electrical controllability during use or high force outputs in both directions of movement.

Future research will focus on observing force output, drawn current and power; Moreover, alternative configurations will be attempted further. It is believed that this approach will also take advantage of improvements in the chemistry and mechanics of the actuator itself, for operating under water without electrolysis or in air without the risk of dehydration and eliminating the need for neutralization between uses.

## References

- 1) D. J. Leo, "Engineering analysis of smart material systems", John Wiley and Sons, 2007
- 2) H. Asanuma et al., "Proposal of an active composite with embedded sensor", Sci Tech Adv Mat 3 (2002), pp. 209–216.
- 3) K. Asaka et al., "Bending of polyelectrolyte membrane platinum composites by electric stimuli: Part II. Response kinetics", Journal of Electroanalytical Chemistry 480 (2000), pp. 186–198.
- 4) M. Shahinpoor et al., "Ionic Polymer-Metal Composites (IPMC) as Biomimetic Sensors and Actuators", Proceedings of SPIE's 5th Annual International Symposium on Smart Structures and Materials, 1-5 March, 1998, San Diego, California. Paper No. 3324-27.
- 5) S. Nemat-Nasser, "Micromechanics of actuation of ionic polymermetal composites," Journal of Applied Physics, vol. 92, no. 5, pp. 2899–2915, 2002.
- 6) W. Zhang et al., "A New Type of Hybrid Fish-like Microrobot", International Journal of Automation and Computing, Vol.3, No.4, pp.358-365, 2006.
- 7) K. Onishi et al., "The effects of counter ions on characterization and performance of solid polymer electrolyte actuator", Electrochim. Acta 46 (2001), pp. 1233–1241.
- 8) H. Nakadoi et al., "Control of Combined IPMC Actuator with 2 Variously Doped Films Experimental Evaluation", Proc. of CCA2007 (2007)
- 9) A. J. McDaid et al., "A conclusive scalable model for the complete actuation response for IPMC transducers", Smart Materials and Structures, 19 (7), 075011, 2010.
- 10) C.K. Landrock et al., "New Capacitive Storage Device", pages 360-363, Proceedings Power MEMS, (2009).
- 11) J. Rossiter et al., "A self-switching bistable artificial muscle actuator", Proceedings of the SICE-ICASE International Joint Conference, 2006
- 12) P. Arena et al., "Design and control of an IPMC wormlike robot", IEEE Trans. Syst. Man Cybern. Part B-Cybern. 36 (5) (2006), pp. 1044–1052.
- 13) K. Oguro et al., "Bending of an ion-conducting polymer film-electrode composite by an electric stimulus at low voltage," Journal of Micromachine Society, 5, 27-30, 1992. (in Japanese)
- 14) J.H. Jeon et al., "Fabrication and actuation of ionic polymer metal composites patterned by combining electroplating with electroless plating", Compos Pt A Appl Sci Manuf 39 (4) (2008), pp. 588–596.
- 15) Z. Chen et al., "Monolithic fabrication of ionic polymer–metal composite actuators capable of complex deformation", Sensors and Actuators A
- 16) S. Yeom et al., "A biomimetic jellyfish robot based on ionic polymer metal composite actuators", Smart Mater. Struct. 18, 2009.
- 17) C. Bonomo et al., "A sensor-actuator integrated system based on IPMCs" Sensors. IEEE. vol. 1 pp.489-492, 2004
- 18) A. Punning et al., "A self-sensing ion conducting polymer metal composite (IPMC) actuator", Sens. Actuators A: Phys. 136 (2) (2007), pp. 656–664.

- 19) B. Kim et al., "A biomimetic undulatory tadpole robot using ionic polymer–metal composite actuators", *Smart Mater. Struct.* 14 (6) (2005), pp. 1579–1585.
- 20) K. Takagi et al., "Development of a rajiform swimming robot using ionic polymer artificial muscles," *Proceedings of the 2006 IEEE/RSJ International Conference on Intelligent Robots and Systems*, pp. 1861–1866, 2006.
- 21) N. Kamamichi et al., "A Snake-like Swimming Robot using IPMC Actuator/Sensor". *ICRA 2006*: 1812-1817
- 22) S. Lee et al., "Designs of IPMC actuator-driven valve-less micropump and its flow rate estimation at low Reynolds numbers", *Smart Mater. Struct.* 15 (2006), p. 1103.
- 23) F. B. Kai et al., "Development of sensing/actuating ionic polymer-metal composite (IPMC) for active guide-wire system", *Sensors and actuators A: physical* pp:1-9
- 24) K. Asaka et al., "Bending of polyelectrolyte membrane-platinum composite by electric stimuli III: self-oscillation", *Electrochimica Acta*, 45(27), pp.4517-4523 (2000)
- 25) D. Kim et al., "Self-oscillating electroactive polymer actuator," *Applied Physics Letters*, 90, 184104, 2007
- 26) M. Yamakita et al. "Control of Biped Walking Robot with IPMC Linear Actuator," *Proc. of IEEE/ASME International Conference*, pp.48-53, 2005.
- 27) C. Yeh et al., "Effects of water content on the actuation performance of ionic polymer–metal composites," *2010 Smart Mater. Struct.* 19
- 28) J. H. Jeon et al., "Snap-through dynamics of buckled IPMC actuator," *Sensors and actuators A: physical* pp:300-305
- 29) H. Chai, "The post-buckling response of a bi-laterally constrained column," *J. Mech. Phys. Solids* 46 7 (1998), pp. 1155–1181
- 30) J. Wang et al., "A highly flexible polymer fiber battery," *J. Power Sources* 150 223–8, 2005

## Acknowledgements

I would like to thank the Japanese Ministry of Education, Culture, Sports, Science and Technology for providing financial support during my undergraduate studies.

It is a pleasure to thank Prof. Hiroshi Asanuma, my advisor, for suggesting the theme for this research and supporting my aspirations of proceeding to graduate school. I also thank Prof. Mitsuji Hirohashi, Dr. Hideo Koyama, Dr. Kenichi Kobayashi, Dr. Takaomi Itoi and Dr. Yun Lu.

It is a pleasure to thank those who made this research possible by providing the sample materials, Dr. Kinji Asaka and Prof. Mohsen Shahinpoor.

I owe my deepest gratitude to Shun Sato for the many productive discussions and remarkable patience. I'd also like to thank my seniors Tomohiro Suzuki, Shuko Ishibashi and Tetsuhiro Mizuno, as well as my colleagues Daisuke Ishiwata, Naoto Shoyama and Takumi Yamashita for the support and understanding.

I am indebted to my parents, Cláudio and Marilda Poubel and my brother Vinícius for the understanding and trust in allowing me to conduct my studies far away from Brazil.

Special thanks are extended to all my friends in Japan for the moral support throughout this research, in particular for Jose Gonzalez for taking the time to check the full paper and to María José Cornejo for the constant emotional support.